Non-equilibrium Dynamics of One-dimensional Many-body Quantum Systems

Thesis Submitted in Partial Fulfillment of the Requirements of the Jay and Jeanie Schottenstein Honors Program

Yeshiva College
Yeshiva University
May 2017

Jonathan Karp

Mentor: Dr. Lea F. Santos, Department of Physics

In this undergraduate honors thesis, I discuss my research in many-body quantum systems far from equilibrium. I start out by giving an accessible introduction to the topic and some motivation for its study. In section II, I give an explanation of how we use computers to represent the interactions and dynamics of many-body quantum systems numerically. In section III, I move on to give a brief introduction to systems of spin-½ particles, which are paradigmatic of many body quantum systems. In section IV, I discuss systems with only two excitations that interact according to the Heisenberg model. The systems are simple, so they can provide valuable insight into the nature of the different terms of the Heisenberg model and the dynamic behavior of spin systems. This insight is helpful for section V, where I discuss complex sytems with many excitations and compare results from integrable and chaotic models to results from using full random matrices. In section VI, I give a qualitative introduction to our current research focus on systems with disorder. Finally, In the appendix, I provide some Python codes for those interested in reproducing the results and further studying the subject.

Contents

I. BACKGROUND AND MOTIVATION

The broad goal of this research program is to advance our understanding of the behavior of many-body quantum systems out of equilibrium, a subject that is at the forefront of theoretical and experimental physics. To better explain what this topic of investigation means, I will start by explaining what we mean by "quantum systems," then move on to justify why our systems of interest are referred to as "many-body." Finally, I will explain what we mean by "far from equilibrium," and why this makes things much more difficult yet more exciting, due to the close connection with potential technological applications.

A. Quantum Systems

In physics, we usually describe our objects of study as systems. A system is just a group of objects whose interactions and dynamics are described by the laws of physics. For example, we could consider the simple system of two stars, and we would describe the gravitational interaction between the stars and their relative motion. Studying quantum systems works similarly, but with the added complications that quantum mechanics is probabilistic and because of the concept of superposition of states.

To understand the probabilistic nature of quantum mechanics, consider by analogy a simple coin flip. Imagine that you flip a coin but don't look at it. If someone were to ask you to describe the state of the coin, you might say that the coin displays heads with 50% probability and tails with 50% probability. You know perfectly well that the actual reality is that it is either heads or tails, but you can only describe the system with probabilities because of your ignorance of the reality.

In quantum mechanics, the two states of a two-level system can be understood analogously to the coin, but with an added wrinkle. Examples of two-level quantum systems include the two spin states of a single spin-½ particle, such as an electron, proton, or neutron; the left or right circular

polarization of a photon; and two energy levels of an atom. If you measure the spin of an electron with respect to a given axis, there are only two possible outcomes, which are often referred to as "spin-up" and "spin-down" and represented by $|\uparrow\rangle$ and $|\downarrow\rangle$, respectively. Before you measure the spin, you can only describe the state with probabilities. However, because we are dealing with a quantum system, there is an extra complication. The probability does not just reflect our ignorance of the reality, but it reflects the actual reality. Quantum mechanics is an intrinsically probabilistic theory. Before the measurement, the system is not in one state or the other, it is said to be in a superposition of both states at the same time [1]. Formally, using the mathematical language of linear algebra, this is described with the so-called wavefunction, denoted by $|\Psi(t)\rangle$ and expressed as a linear combination of the two possible spin states, as:

$$|\Psi(t)\rangle = c_1(t)\,|\uparrow\rangle + c_2(t)\,|\downarrow\rangle\,. \tag{1}$$

The coefficients $c_1(t)$ and $c_2(t)$ are the probability amplitudes of spin-up and spin-down respectively, and their values can depend on time. When the spin of the electron is measured at time t, the result will be spin-up with probability $|c_1(t)|^2$ and spin-down with probability $|c_2(t)|^2$.

B. Many-Body Quantum Systems

If we consider a system of two interacting spin ½ particles, it is impossible to describe the state of a single particle without considering the other, so we can only look at states of the system as a whole. We then have to consider four separate possible states: $|\uparrow\rangle\,|\uparrow\rangle$, $|\uparrow\rangle\,|\downarrow\rangle$, $|\downarrow\rangle\,|\uparrow\rangle$, and $|\downarrow\rangle\,|\downarrow\rangle$, and the wavefunction is expressed as a linear combination of these four states. For a system of N interacting spins-½, the number of possible states is 2^N, all embedded in a single wavefunction. We investigate the time evolution of systems with more than 10 particles, which results in very large wavefunctions. The behavior of systems of single particles has been understood for the past 90 years, but the behavior of some many-body quantum systems is still not well understood. These systems are so complicated that it is often impossible to treat them analytically, so we need to resort to numerical methods in the hopes of gaining some insight into how they behave. Although, even employing numerical methods for this problem is challenging. Since the number of states increases exponentially with system size, we lack the computational resources to deal with even moderately small systems, as we soon run out of memory.

C. Non-equilibrium Many-Body Quantum Dynamics

When we say that a system is out of equilibrium, we mean that the state of the system changes in time. There are well established methods involving Linear Response Theory [2] for dealing with systems at or very close to equilibrium, but these methods do not apply to systems that are far from equilibrium. In the long run, we hope to be able to understand and give a precise characterization to the dynamics of these systems from their initial states until they reach equilibrium.

D. Motivation

There are three main motivators for our striving to reach a better understanding of many-body quantum systems out of equilibrium. First off, it is a fundamental problem of great interest to physical sciences. Understanding the properties of interacting many-body quantum systems out of equilibrium is central to a wide range of fields, from atomic, molecular, and condensed matter physics to quantum information and cosmology [3].

Additionally, these systems are now experimentally accessible due to the remarkable recent experimental progress in evolving and controlling the evolution of isolated complex quantum systems, in particular with cold atoms in optical lattices [4] and trapped ions [5, 6]. These experiments can validate or discard theoretical studies and can also open up new scenarios of investigation. Theorists and experimentalists have been working in tandem and in a symbiotic relationship, building off of each other's work to develop a rigorous and comprehensive understanding of the behavior of non-equilibrium many-body quantum systems.

Finally, these studies carry the potential for enabling a variety of technological applications. Some are mentioned below.

⇒ The analysis of non-equilibrium quantum dynamics may reveal new phases of matter that typically do not occur near equilibrium, which can permit the development of new materials.

⇒ The models employed to describe many-body quantum systems are directly related to those in the field of quantum computing [7]. A normal computer stores information in bits, each of which is physically represented by a parallel plate capacitor. The capacitor, like the coin, has only two possible states: charged or uncharged, 1 or 0. Each bit can only hold that one piece of information, and each bit is independent of the others. A quantum computer stores information in qubits, each of which can be represented by a spin ½ particle. Each qubit can be in a superposition of two possible states, so the system with N qubits can be in a superposition of 2^N states, and these qubits may be correlated. Computations can be done on multiple states at the same time, which is known as *quantum parallelism*, dramatically reducing the time required to carry out computations. Advances in our understanding of many-body quantum systems can lead to revolutionary developments in both computational capabilities and encryption technologies. Ironically, one of the important benefits of quantum computers is that they could be used to simulate large many-body quantum systems. Quantum computers would make the study of many-body quantum systems much easier, but quantum computers are themselves many-body quantum systems, so it is hard to build quantum computers without a rigorous understanding of many-body quantum systems.

⇒ Improvements in transporting heat rapidly to combat the effects of local heating are necessary for the development of new electronic devices. Being able to control the transport of excited spin states is also instrumental in the development of spintronic devices, where information is transferred through exchange of spins instead of charges, and therefore is better protected against dissipation.

II. NUMERICAL REPRESENTATION OF QUANTUM SYSTEMS

A. Basis

The systems that we will be dealing with are one dimensional arrays of spin ½ particles. In order to represent the wavefunctions for these systems as linear combinations of possible states, we must choose a basis. While there are technically an infinite number of possible choices for the basis, the natural choice is the so called "site basis" or "computational basis." In this basis, each vector represents a state where the spin of each site is determined, so it is either pointing up or down with respect to a certain direction. Computationally, if there are N sites, we can represent each vector as a list of N 0s and 1s, where 1 represents spin-up and 0 represents spin-down. Codes for generating the basis are given in the appendix.

B. Hamiltonian

Once we have a basis, we can construct the Hamiltonian. The Hamiltonian, denoted $\hat{H}$, is an operator representing the total energy of the system. It gives details about the number of particles

in the system and how they interact. It also specifies the size, symmetries, geometry, and phase of the system, as well as if it has impurities or not. For discrete systems, such as the spin systems that we study, the Hamiltonian is a matrix of dimension $\mathcal{D} = 2^N$, equal to the number of basis vectors. In most of the cases that we study, the total number r of spins-up is conserved, so the Hamiltonian is composed of independent blocks, each of dimension:

$$\mathcal{D} = \binom{N}{r} = \frac{N!}{r!(N-r)!} \tag{2}$$

Therefore, we are often dealing only with one subspace of the system at a time, allowing us to study larger system sizes.

Once we have the Hamiltonian in the site basis, we can diagonalize it to obtain the eigenvalues and the eigenvectors. The eigenvalues are the allowed energies of the system and the eigenvectors form a basis of states of deterministic energy. Additionally, the structure of the eigenvalues and eigenvectors can give us information about how the system will behave in time.

There are many factors to take into account when constructing the Hamiltonian, and we are interested in the effects of these factors on the eigenvalues, eigenvectors, and the dynamics of the system. These factors include:

⇒ The strength and range of the interactions. We start by considering simple systems where the only particles that interact are those in nearest neighbor sites. We then consider interactions between next-nearest neighbor sites and faraway sites. We are interested in both how the presence of faraway interactions and the strength of faraway interactions relative to nearest neighbor interactions affect the properties of the system.

⇒ The ratio of spins up to spins down. The behavior of a dilute system may be very different from that of a system in the dense limit. When the number of spins-up and down are similar, the system may exhibit stronger signatures of quantum chaos [10].

⇒The number of spins-up that interact simultaneously. In most condensed matter systems, including the systems that we study, there are only two-body interactions, that is, only two particles interact at the same time. In nuclear systems, however, we often find simultaneous interactions between three particles.

⇒ The geometry of the system. When we work with one dimensional arrays of quantum particles, we can consider systems where the sites are in a line, which we call open boundary conditions, or we can consider systems where the sites are arranged in a ring, which we call closed or periodic boundary conditions.

⇒ The dimension of the system. We focused specifically one one-dimensional systems, but many people are also studying two and three-dimensional systems.

⇒ The presence of disorder. Any real system has has impurities and imperfections that may translate into different onsite energies and coupling strengths. We represent a disordered system by using random numbers to describe the onsite energies. For each observable quantity, we average the result over many disorder realizations.

An example Hamiltonian code with closed boundary conditions, nearest neighbor and next nearest neighbor coupling, and defects is given in the appendix.

C. Wavefunction

After constructing the Hamiltonian, which represents all of the interactions in the system, we can determine the dynamics of the system. All information about a quantum system and its evolution is contained in the wavefunction, which can be found by solving the Schrödinger equation [1]:

$$i\hbar \frac{\partial |\Psi\rangle}{\partial t} = \hat{H} |\Psi\rangle , \tag{3}$$

where i is the imaginary unit and $\hbar$ is the reduced Planck constant. This is a partial differential equation, whose solution is highly non-trivial. Even so, since the Hamiltonians we deal with do not depend explicitly on time, we can use separation of variables [1], yielding the stationary states:

$$|\Psi_j(t)\rangle = \exp\Big(-i\frac{E_j t}{\hbar}\Big)\,|\psi_j\rangle \tag{4}$$

where $|\psi_j\rangle$ are solutions to the time independent Schrödinger equation[1]:

$$\hat{H}\,|\psi_j\rangle = E_j\,|\psi_j\rangle \tag{5}$$

which is an eigenvalue equation with each E_j being an eigenvalue of $\hat{H}$ with corresponding eigenvector $|\psi_j\rangle$. We can then use computer software to find the eigenvalues and eigenvectors. Like all operators representing observables, the Hamiltonian is a Hermitian operator, so its eigenvalues are real and its eigenvectors span the vector space [1]. The general solution to the Schrödinger equation can then be written as a linear combination of stationary states[1]:

$$|\Psi(t)\rangle = \sum_{j=1}^{\mathcal{D}} c_j \exp\Big(-i\frac{E_j t}{\hbar}\Big)\,|\psi_j\rangle \tag{6}$$

where $\mathcal{D}$ is the dimensionality of the vector space. If the eigenvalues are not degenerate, then the normalized eigenvectors will be mutually orthogonal. If there are degeneracies, then the eigenvalues can still be made orthogonal by using the Gram-Schmitt orthogonalization process[1], which most computational software used to compute eigensystems will do automatically. Once we have a set of orthonormal eigenvectors, the coefficients c_j are the projections of the eigenvectors on the initial state[1]:

$$c_j = \langle\psi_j\,|\,\Psi(0)\rangle \tag{7}$$

This can be simplified if we assume that the initial state of the system is one of the site basis vectors. Let $|\phi_k\rangle$ denote the site basis and set $|\Psi(0)\rangle = |\phi_{ini}\rangle$. Writing the eigenvectors in terms of the site basis, we have:

$$|\psi_j\rangle = \sum_{k=1}^{\mathcal{D}} a_k^{(j)}\,|\phi_k\rangle \tag{8}$$

The expression for c_j becomes:

$$c_j = \langle\psi_j\,|\,\phi_{ini}\rangle = a_{ini}^{(j)} \tag{9}$$

The wavefunction can then be written as [8]:

$$|\Psi(t)\rangle = \sum_{j=1}^{\mathcal{D}} a_{ini}^{(j)} \exp\Big(-i\frac{E_j t}{\hbar}\Big)\,|\psi_j\rangle = \sum_{k=1}^{\mathcal{D}} \left(\sum_{j=1}^{\mathcal{D}} a_{ini}^{(j)} a_k^{(j)} \exp\Big(-i\frac{E_j t}{\hbar}\Big)\right)|\phi_k\rangle \tag{10}$$

and the probability of finding the system in the state $|\phi_k\rangle$ as a function of time is:

$$P_k(t) = \left|\sum_{j=1}^{\mathcal{D}} a_{ini}^{(j)} a_k^{(j)} \exp\Big(-i\frac{E_j t}{\hbar}\Big)\right|^2 \tag{11}$$

Code for finding the wavefunction and probabilities is given in the appendix.

III. SPIN SYSTEMS

A. Spin Operators

The spin of a single particle can be represented by the spin operators $\hat{S}^{x,y,z} = \frac{\hbar}{2}\hat{\sigma}^{x,y,z}$[1], where $\hat{\sigma}^{x,y,z}$ are the Pauli matrices:

$$\hat{\sigma}^x = \begin{pmatrix} 0 & 1 \\ 1 & 0 \end{pmatrix}, \quad \hat{\sigma}^y = \begin{pmatrix} 0 & -i \\ i & 0 \end{pmatrix}, \quad \hat{\sigma}^z = \begin{pmatrix} 1 & 0 \\ 0 & -1 \end{pmatrix} \tag{12}$$

For convenience, we set $\hbar = 1$. The quantum state of the spin can be represented by a two component vector called a spinor, typically written in terms of the eigenvectors of $\hat{\sigma^z}$: $|\uparrow\rangle = \binom{1}{0}$ and $|\downarrow\rangle = \binom{0}{1}$, what we call spin-up and spin-down. The eigenvalue of $\hat{\sigma}^z$ corresponding to $|\uparrow\rangle$ is 1, and the eigenvalue corresponding to $|\downarrow\rangle$ is -1, so spin-up has higher energy and is therefore referred to as the excitation.

B. Heisenberg Model

Let us consider a simple one-dimensional spin chain with open boundary conditions, only nearest neighbor interactions, and no disorder. This system can be represented with the XXZ Heisenberg model, given by [9]:

$$\hat{H}_{XXZ} = \sum_{n=1}^{N-1} \left[J\Delta \hat{S}_n^z \hat{S}_{n+1}^z + J(\hat{S}_n^x \hat{S}_{n+1}^x + \hat{S}_n^y \hat{S}_{n+1}^y) \right] \tag{13}$$

where N is the number of sites in the chain, the operator $\hat{S}_n^z$ acts only on site n, J is a parameter that gives the energy scale which we set to 1 in our codes, and Δ is the anisotropy parameter, a measure of the relative strength of the two coupling terms. We make Δ an argument of the function for the Hamiltonian in our codes.

The first term in the Hamiltonian is the Ising interaction. The effect of the Ising term can be demonstrated with the Ising terms action on the four possible orientations of two spins:

$$\begin{aligned} J\Delta \hat{S}_n^z \hat{S}_{n+1}^z |\uparrow_n\uparrow_{n+1}\rangle &= \frac{J\Delta}{4} |\uparrow_n\uparrow_{n+1}\rangle \\ J\Delta \hat{S}_n^z \hat{S}_{n+1}^z |\downarrow_n\downarrow_{n+1}\rangle &= \frac{J\Delta}{4} |\downarrow_n\downarrow_{n+1}\rangle \\ J\Delta \hat{S}_n^z \hat{S}_{n+1}^z |\uparrow_n\downarrow_{n+1}\rangle &= -\frac{J\Delta}{4} |\uparrow_n\downarrow_{n+1}\rangle \\ J\Delta \hat{S}_n^z \hat{S}_{n+1}^z |\downarrow_n\uparrow_{n+1}\rangle &= -\frac{J\Delta}{4} |\downarrow_n\uparrow_{n+1}\rangle \end{aligned} \tag{14}$$

We see that, for $\Delta > 0$, the Ising term causes a pair of parallel spins to have a higher energy than a pair of anti-parallel spins. Additionally, since $\hat{S}^z$ does not change the orientation of the spins, the Ising term only affects the diagonal term of the Hamiltonian matrix. Therefore, the Ising interaction defines the energy of each basis vector but does not contribute to the dynamics of the system.

The second term in the Hamiltonian is referred to as the flip-flip term.

$$\begin{aligned} J(\hat{S}_n^x \hat{S}_{n+1}^x + \hat{S}_n^y \hat{S}_{n+1}^y) |\uparrow_n\downarrow_{n+1}\rangle &= \frac{J}{2} |\downarrow_n\uparrow_{n+1}\rangle \\ J(\hat{S}_n^x \hat{S}_{n+1}^x + \hat{S}_n^y \hat{S}_{n+1}^y) |\downarrow_n\uparrow_{n+1}\rangle &= \frac{J}{2} |\uparrow_n\downarrow_{n+1}\rangle \end{aligned} \tag{15}$$

The flip-flip term does not affect parallel spins:

$$\begin{aligned} J(\hat{S}_n^x \hat{S}_{n+1}^x + \hat{S}_n^y \hat{S}_{n+1}^y) \left|\uparrow_n \uparrow_{n+1}\right\rangle = 0 \\ J(\hat{S}_n^x \hat{S}_{n+1}^x + \hat{S}_n^y \hat{S}_{n+1}^y) \left|\downarrow_n \downarrow_{n+1}\right\rangle = 0 \end{aligned} \tag{16}$$

The flip-flip term defines the off-diagonal terms, and it causes the system to evolve in time by moving excitations through the chain. It is clear that the Heisenberg model conserves the number of excitations.

In principle, we should add another term to the Hamiltonian corresponding to the energy of each site. The term would be:

$$\sum_{n=1}^{N} \epsilon_n \hat{S}_n^z \tag{17}$$

and it corresponds to the Zeeman splitting of each site due to a static external magnetic field acting on that site. However, if we assume that the sites are all identical, then we do not have to include this term. Since each basis vector contains the same number of spins-up and spins-down, the term would just add the same constant to each diagonal term of the Hamiltonian, which would not affect the dynamics. In case of defects or disorder that makes the energy due to Zeeman splitting different on different sites, then we would have to include this term in the Hamiltonian.

IV. SYSTEMS WITH TWO EXCITATIONS

A. Doublons

1. *Diagonal Terms*

I started my analysis with simple cases of the Heisenberg XXZ model where the systems have two excitations. Since the Ising term causes a pair of parallel spins to have greater energy than a pair of anti-parallel spins, the Ising term tries to keep the two up-spins together in a bound state called a *doublon* [11, 12]. We are interested in analyzing the behavior of these doublons. The first step is to look at the diagonal terms of the Hamiltonian, each of which corresponds to the energy of a basis vector and is given by the Ising term. For each basis vector, the corresponding energy can be found by adding $J\Delta/4$ for each pair of parallel spins and subtracting $J\Delta/4$ for each pair of antiparallel spins.

For example, consider a case with 8 sites, open boundary conditions, and the basis vector $|00110000\rangle$, which has a doublon. Figure 1 (a) shows that the vector has five pairs of parallel spins and two pairs of antiparallel spins, for a total energy of $\frac{5J\Delta}{4} - \frac{2J\Delta}{4} = \frac{3J\Delta}{4}$.

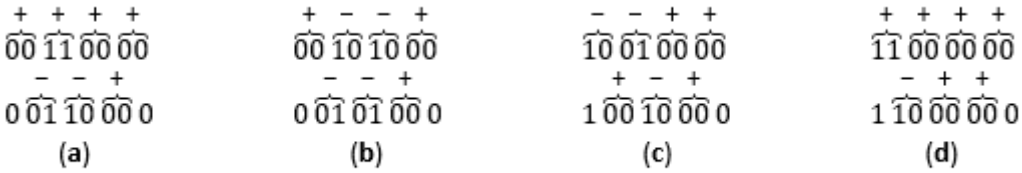

FIG. 1: The Ising interaction of four example basis vectors

Next, consider a vector without a doublon: $|00101000\rangle$ (Figure 1 (b)). The vector has three pairs of parallel spins and four pairs of anti-parallel spins, for a total energy of $\frac{3J\Delta}{4} - \frac{4J\Delta}{4} = \frac{-J\Delta}{4}$. We see that the vector with the doublon was a higher energy than the one without a doublon. The energy difference increases with increasing Δ, so for high values of Δ the flip-flop term will not be able to couple vectors with doublons to vectors without doublons. Therefore, for high values of Δ, a doublon will stay together. For large systems with two excitations, a vast majority of basis vectors do not contain doublons.

When we deal with open boundary conditions, we must also consider border effects. Consider the vector $|10010000\rangle$, with an excitation on the border (Figure 1 (c)). The vector has four pairs of parallel spins and three pairs of antiparallel spins, for a total energy of $\frac{4J\Delta}{4} - \frac{3J\Delta}{4} = \frac{J\Delta}{4}$. This vector has energy halfway between a vector without a doublon or excitation on the border and a vector containing a doublon outside the border. This shows that having an excitation on the border has half of the energy of a doublon. The vector $|10000001\rangle$, with excitations on both borders, has the same energy as a vector containing a doublon. It is more likely that the flip-flop term will be able to couple vectors with doublons outside but close to the border to vectors with an excitation on the border than to vectors with split excitations away from the border. Additionally, the vector $|10000001\rangle$ could be coupled with doublons no matter how strong the Ising interaction is. We see that using open boundary conditions makes it easier for doublons to be split.

Finally, consider the vector $|11000000\rangle$ (Figure 1 (d)), which contains a doublon on the boundary. The vector has six pairs of parallel spins and one pair of antiparallel spins, for a total energy of $\frac{6J\Delta}{4} - \frac{J\Delta}{4} = \frac{5J\Delta}{4}$. We see that the energy boost over an ordinary vector is the boost for a doublon plus the energy boost for an excitation on the border.

This same behavior holds for chains of any size. Vectors without doublons or excitations on the border have the lowest energy. $\frac{J\Delta}{2}$ is added to the energy for each spin-up on the boundary, and $J\Delta$ is added if the vector contains a doublon. In general, for systems with open boundary conditions, two excitations, only nearest neighbor interactions, and no disorder, there will be only four different diagonal terms in the Hamiltonian.

2. Eigenvalues and Eigenvectors

The next step is to look at the eigenvalues and eigenvectors of the Hamiltonian. The eigenvectors are certain linear combinations of site basis vectors, and they are deterministic states of energy. The eigenvalues associated with each eigenvector is that energy. For low values of Δ, the flip-flop term is able to couple any basis vectors together, so the eigenvectors are large superpositions with significant participation of many basis vectors and the eigenvalues form a broad spectrum around the energies of the basis vectors. For high values of Δ, the flip-flip term cannot couple basis vectors of different energies. Consequently, each eigenvector is composed of just states of the same energy and the corresponding eigenvalues have energies close to that energy.

For a simple example, we will consider a very small system with just four sites. Since the system is so small, the border effects play a large role. Therefore, we use closed boundary conditions so that we do not have to worry about border effects. In this case, the basis vectors are: $|1100\rangle$, $|1010\rangle$, $|1001\rangle$, $|0110\rangle$, $|0101\rangle$, $|0011\rangle$. Since we are using closed boundary conditions, $|1001\rangle$ has a doublon.

For $\Delta = .1$, the Hamiltonian matrix is given by:

$$H = \begin{pmatrix} 0 & .5 & 0 & 0 & .5 & 0 \\ .5 & -.1 & .5 & .5 & 0 & .5 \\ 0 & .5 & 0 & 0 & .5 & 0 \\ 0 & .5 & 0 & 0 & .5 & 0 \\ .5 & 0 & .5 & .5 & -.1 & .5 \\ 0 & .5 & 0 & 0 & .5 & 0 \end{pmatrix} \tag{18}$$

Note that there are only two different diagonal terms: 0 corresponding to a vector with a doublon, $-.1$ corresponding to a vector without a doublon. The difference between these two energies is less than the off diagonal terms, which are all .5, so the flip-flop interaction will be able to couple any basis vectors together.

In this case, the eigenvalues of the Hamiltonian (rounded to two decimal places) are: -1.47, -0.1, 0, 0, 0, 1.37. The Matrix with eigenvectors as columns (also rounded to two decimal places) is:

$$\begin{pmatrix} .35 & 0 & .87 & 0 & 0 & .36 \\ -.51 & -.71 & 0 & 0 & 0 & .49 \\ .35 & 0 & -.29 & -.58 & -.58 & .36 \\ .35 & 0 & -.29 & -.21 & -.79 & .36 \\ -.51 & .71 & 0 & 0 & 0 & .49 \\ .35 & 0 & -.29 & .79 & -.21 & .36 \end{pmatrix} \tag{19}$$

We see that some of the eigenvalues are not close to the diagonal terms in the Hamiltonian, and some of the eigenvectors have significant probability amplitudes for both vectors with doublons and vectors without doublons.

In the case of $\Delta = 10$, the Hamiltonian is the same as the previous case, but with the diagonal terms multiplied by 100.

$$H = \begin{pmatrix} 0 & .5 & 0 & 0 & .5 & 0 \\ .5 & -10 & .5 & .5 & 0 & .5 \\ 0 & .5 & 0 & 0 & .5 & 0 \\ 0 & .5 & 0 & 0 & .5 & 0 \\ .5 & 0 & .5 & .5 & -10 & .5 \\ 0 & .5 & 0 & 0 & .5 & 0 \end{pmatrix} \tag{20}$$

The eigenvalues of the Hamiltonian are: -10.2, -10, 0, 0, 0, .2. All of the eigenvalues are close to either of the diagonal terms in the Hamiltonian. The matrix with eigenvectors as columns (rounded to two decimal places) is:

$$\begin{pmatrix} -.07 & 0 & 0 & 0 & .87 & -.5 \\ .7 & .71 & 0 & 0 & 0 & -.1 \\ -.07 & 0 & -.58 & -.29 & -.58 & -.5 \\ -.07 & 0 & .79 & -.29 & -.79 & -.5 \\ .7 & -.71 & 0 & 0 & 0 & -.1 \\ -.07 & 0 & -.21 & -.29 & -.21 & -.5 \end{pmatrix} \tag{21}$$

The first two eigenvectors, with corresponding eigenvalues close to the energies of basis vectors that do not contain doublons, only have significant probability amplitudes for basis vectors that do not contain doublons. Conversely, the last four eigenvectors, with eigenvalues close to the

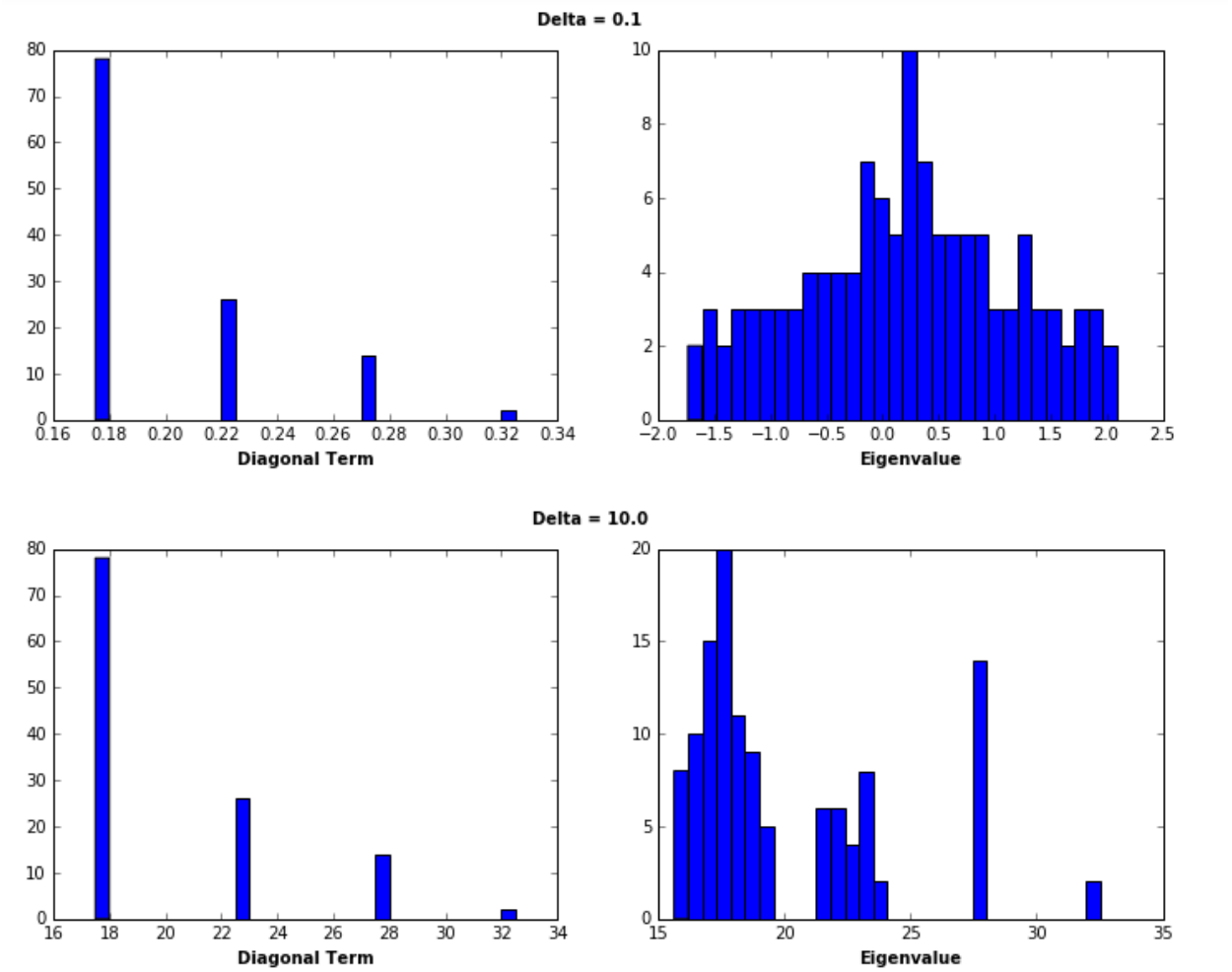

FIG. 2: Histograms of diagonal terms (left) and eigenvalues (right) for $\Delta = .1$ (top) and $\Delta = 10$ (bottom). $N = 16$, 2 up-spins, open boundary conditions.

energies of basis vectors containing doublons, only have significant contributions from basis vectors containing doublons.

For larger systems, we cannot look at the eigenvectors explicitly, as the matrix of eigenvectors is just too large for us to examine carefully, so we employ statistical analysis. We often use histograms to analyze the eigenvalues. Consider a system with 16 sites, two excitations, and open boundary conditions. Figure 2 shows the histograms of the diagonal terms and eigenvalues for $\Delta = .1$ and $\Delta = 10$. For $\Delta = .1$, the eigenvalues span a broad range of energies around the diagonal terms. However, for $\Delta = 10$, the eigenvalues cluster around the energy values of the diagonal terms and separate energy bands are formed.

Since for larger systems only a small percentage of basis vectors contain doublons, for high values of Δ the eigenvectors composed of the basis vectors containing doublons will only involve a small percentage of basis vectors. On the other hand, eigenvectors that do not encompass states with doublons will be spread out in the basis. We are often interested in quantifying how much a given state is spread out in a basis. A common quantity used for this is the so called participation ratio (PR). If a state is written in a particular basis of dimension $\mathcal{D}$ where each basis vector has

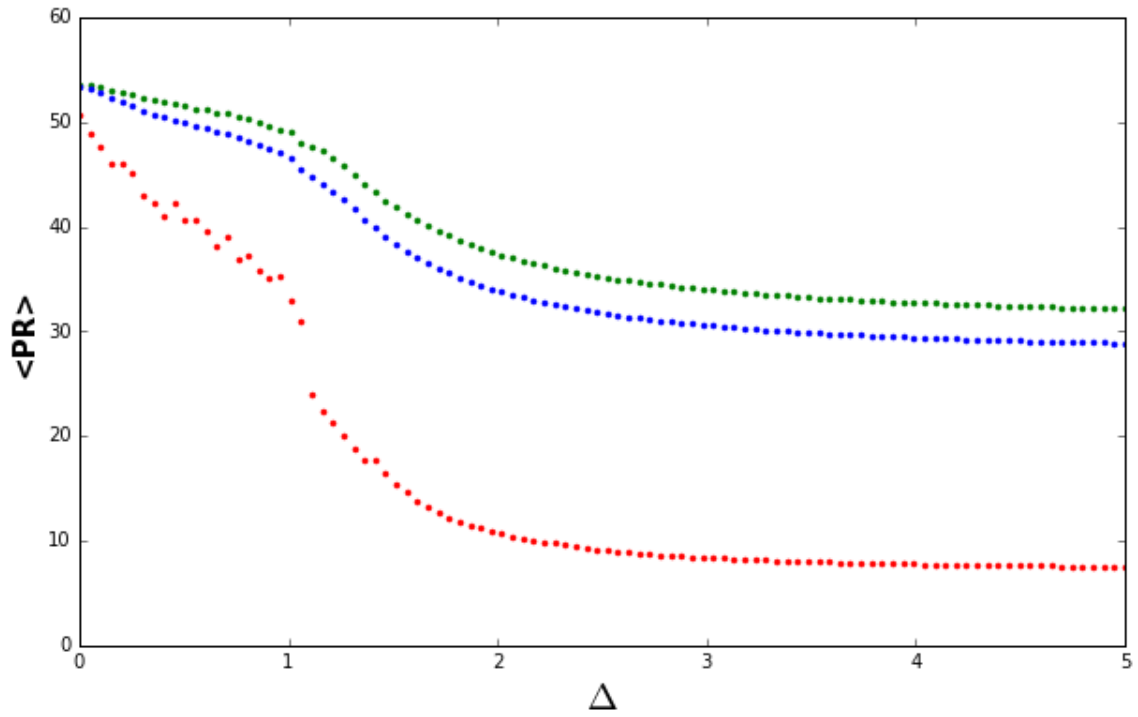

FIG. 3: Average participation ratio for all eigenvectors (blue), eigenvectors containing doublons (red) and eigenvectors that do not contain doublons (green). $N = 16$, 2 up-spins, open boundary conditions.

probability amplitude C_k, then the PR is given by:

$$PR = \frac{1}{\sum_{k=1}^{\mathcal{D}} |C_k|^4} \tag{22}$$

Figure 3 (blue data) shows the average PR over all eigenstates as a function of Δ. As Δ increases, the vectors containing doublons cannot mix with the other vectors, so the eigenvectors become more localized. Note that the largest drop in PR is at around $\Delta = 1$, where the Ising interaction strength is of the order of the flip-flop coupling strength.

I also split between the eigenvectors between those comprised of vectors containing doublons (in red) and those that do not (in green)., I assumed that an eigenvector contains doublons if the total probability of measuring a basis vector with a doublon while in that eigenstate exceeds .2. The average PR for both types of eigenvectors is nearly equal as $\Delta \to 0$. However, as Δ increases, the average PR for eigenvectors encompassing doublons decreases much more quickly, as those eigenvectors become more localized.

3. Dynamics

We have seen that for high values of Δ, doublons stay together, so they can be thought of as single bound states. A doublon moves together as if it is one particle, but it moves slower. Because of superposition of states, it is not so simple to show how quickly the excitations move. One quantity that we use to measure the speed of dynamics is the survival probability W_{ini} , which is the probability that the system will be measured to be in the initial state as a function of time.

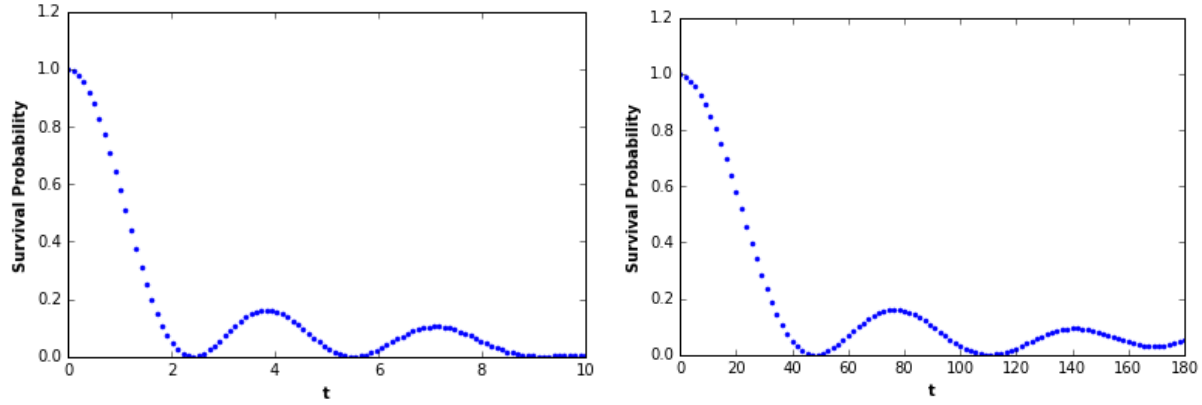

FIG. 4: The graph on the left shows the Survival Probability for a system with 15 sites, one excitation, and initial state $|000001000000000\rangle$. The graph on the right shows the survival probability for 16 sites, two excitations, $\Delta = 10$ and initial state $|0000011000000000\rangle$. Open boundary conditions are used in both cases

From equation (11), the survival probability is given by:

$$W_{ini}(t) = \left| \sum_{j=1}^{\mathcal{D}} |a_{ini}^{(j)}|^2 \exp\Big(-i\frac{E_j t}{\hbar}\Big) \right|^2 \tag{23}$$

Figure 4 shows that the survival probability of the doublon in a case of $N = 16$ and $\Delta = 10$ is virtually the same as for a single excitation with one excitation and $N = 15$, but the time scale for the doublon is much longer. This suggests that a doublon moves as a single excitation, but at a much slower pace. To understand why the doublon moves slower, consider the neighboring doublons $|00001100\rangle$ and $|00011000\rangle$. The flip-flop term can only exchange a spin-up with a spin-down, so it cannot directly couple these terms together. Instead, it must go through the intermediate state $|00010100\rangle$ to get from one to the other. Because of quantum tunneling, the system can be from one doublon to the other without the system actually being in the intermediate state, but it takes some time for that to happen.

We can also use equation (11) to find the probabilities for each basis vector, to get an idea of which vectors play a role in the dynamics. We could plot the probability of measuring each basis vector on the same graph, but even for relatively small systems it becomes very difficult to differentiate between the many curves of the different basis vectors on the graph. Nonetheless, we are usually not interested in individual basis vectors but in certain types of basis vectors. For example, in our case we are interested in whether a vector contains a doublon or not. We then only have to graph the sum of the probabilities of the vectors with doublons and the sum of the vectors without doublons.

For example, consider a system with 8 sites. Figure 5 shows the total probabilities for vectors with and without doublons for $\Delta = .1$ and $\Delta = 10$, where the initial state is $|00001100\rangle$, a vector with a doublon not on the border. For $\Delta = .1$, the doublon is broken apart and vectors without doublons have significant probabilities. Conversely, for $\Delta = 10$, the doublon stays together and only vectors with doublons have significant probabilities.

In the case of $\Delta = 10$, we know that only at most seven vectors play a significant role in the dynamics, so we can then graph the probabilities of those vectors separately. Figure 6 shows the probabilities of the particular vectors with doublons for $\Delta = 10$. The vectors with doublons on the border do not show up in the dynamics, as they have a greater energy than the regular vectors with doublons due to the border effect. Also, the doublon moves away from its original pair of

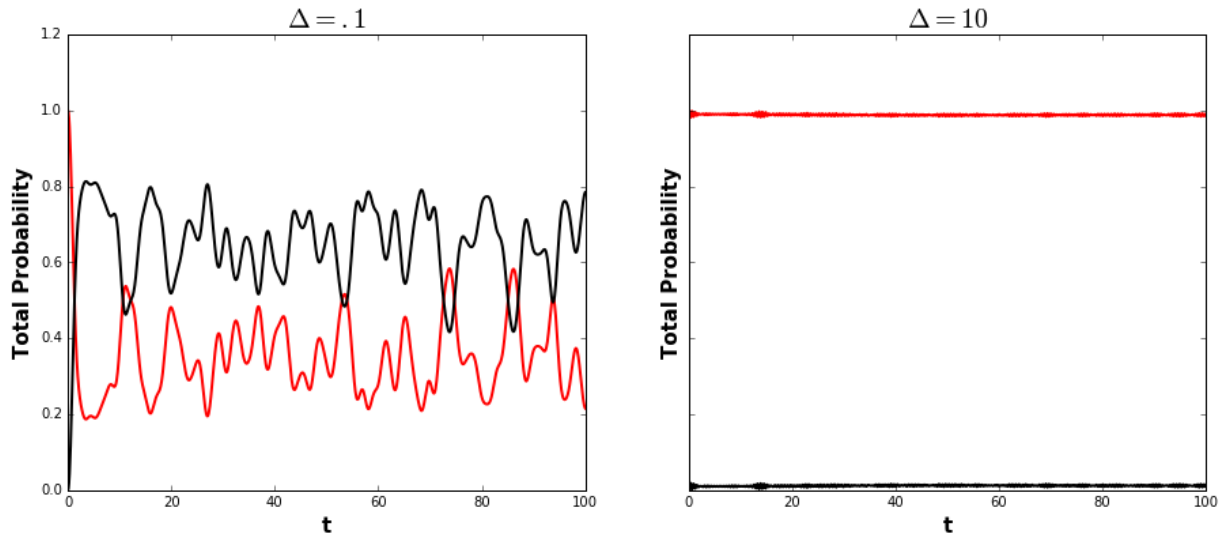

FIG. 5: Total probabilities for basis vectors with doublons (red) and without doublons (black) for $\Delta = .1$ (left) and $\Delta = 10$. $N = 8$, open boundary conditions, and initial state $|00001100\rangle$ are used for both.

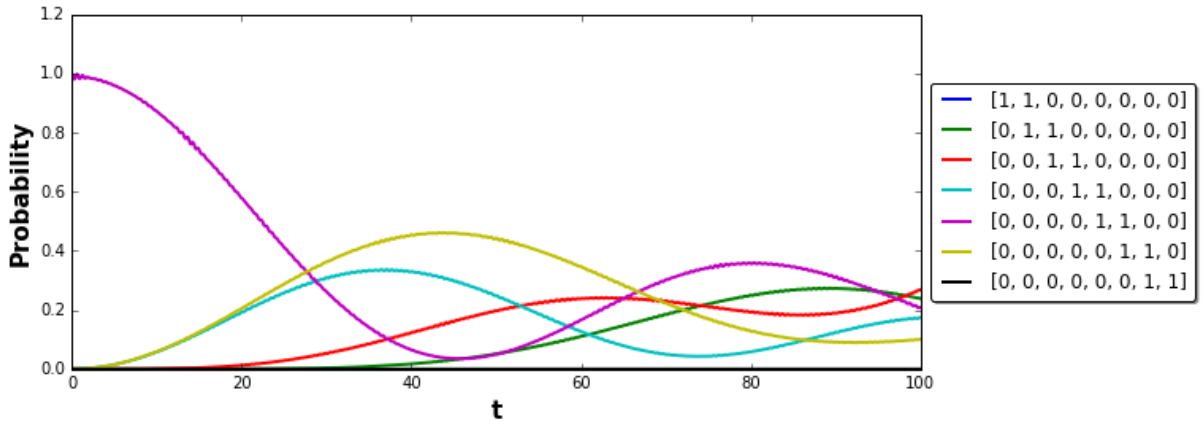

FIG. 6: Probabilities for basis vectors containing doublons. $N = 8$, $\Delta = 10$, open boundary conditions, initial state $|00001100\rangle$.

sites gradually populating other pairs. Starting at sites (5,6), we see first the participation of the neighbors (4,5) and (6,7), subsequently the probability for being on sites (3,4) increases, and finally (2,3) shows up.

It is noteworthy that in the case of $\Delta = 10$, the vector $|10000001\rangle$ does not show up in the dynamics. Even though this vector does not contain a doubloon since we are considering open boundary conditions, it still has the same energy as a vector with a doublon. This shows that energy is not the only consideration in which basis vectors show up in the dynamics. Even though that vector has the same energy as a vector with a doublon, the flip-flop coupling would have to go through many exchanges of spins to get from a doublon to that vector, requiring a large time scale before that vector appears in the dynamics.

This effect can be demonstrated by considering the states $|11000000\rangle$ and $|00000011\rangle$. These states both have the same energy, and a different energy from every other state. If we set $\Delta = 10$ and $|11000000\rangle$ to be the initial state, it will oscillate between those two states, but it will take an

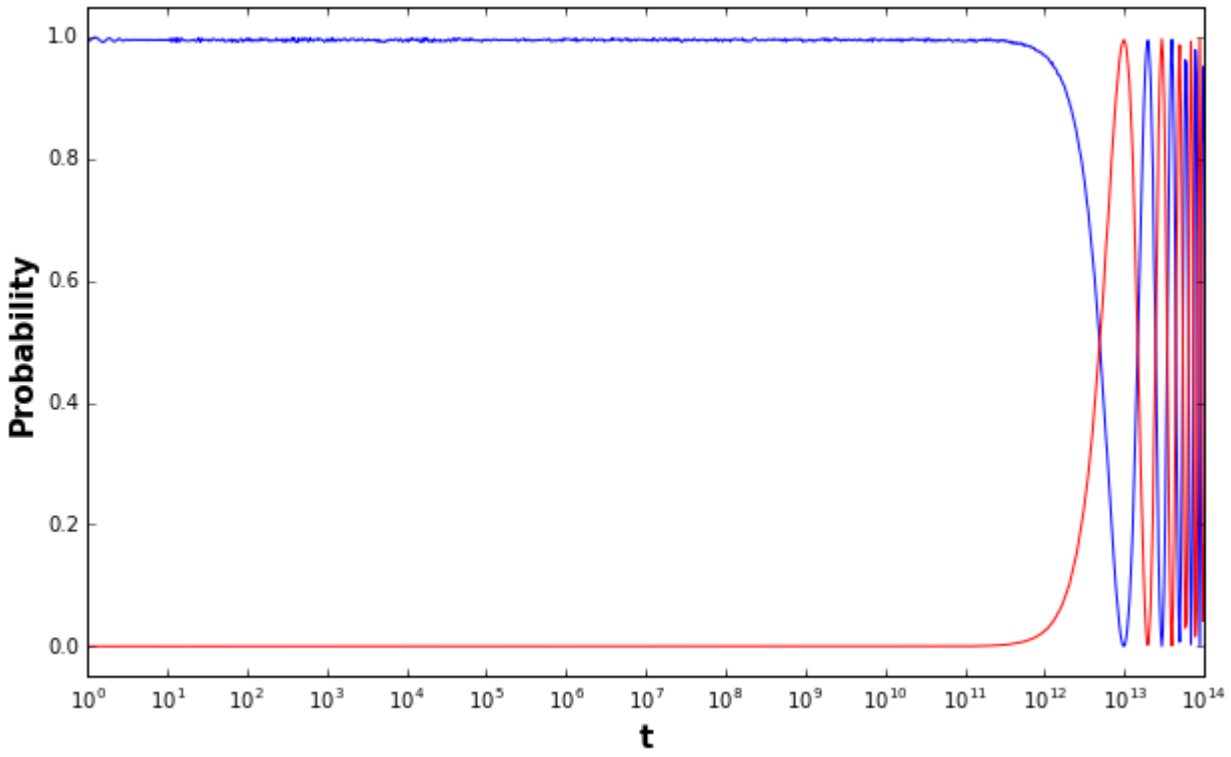

FIG. 7: Probabilities for the initial state $|11000000\rangle$ (blue) and $|00000011\rangle$ (red) as a function of time, where time is on a log scale. $N = 8$, $\Delta = 10$, open boundary conditions.

extremely long time to get from one state to the other, as shown in Figure 7. The figure shows that the system appears to only be in the initial state until time 10^{12}. Thus, practically speaking, the vector $|00000011\rangle$ is not important in the dynamics. This time scale increases with increasing N.

B. Long Range Interactions: Breaking Doublons

We next consider the effect of adding next nearest neighbor (NNN) interactions between the particles. The Hamiltonian with NNN interactions is given by:

$$H = H_{XXZ} + \lambda H_{NNN} \tag{24}$$

where λ is the strength of the NNN couplings relative to the NN couplings and:

$$H_{NNN} = \sum_{n=1}^{N-2} \left[J\Delta \hat{S}_n^z \hat{S}_{n+2}^z + J(\hat{S}_n^x \hat{S}_{n+2}^x + \hat{S}_n^y \hat{S}_{n+2}^y) \right] \tag{25}$$

Figure 8 shows the probabilities of the basis vectors for $\Delta = 10$ where the initial state is a doublon. The panels compare different scenarios, which include the case with just nearest neighbor couplings, NN couplings and NNN flip-flop term, NN couplings and NNN Ising term, NN and NNN couplings.

In the case where there are just nearest neighbor couplings (as in the top left panel of figure 8), only the vectors with doublons show up with significant probabilities, as we saw before. When the

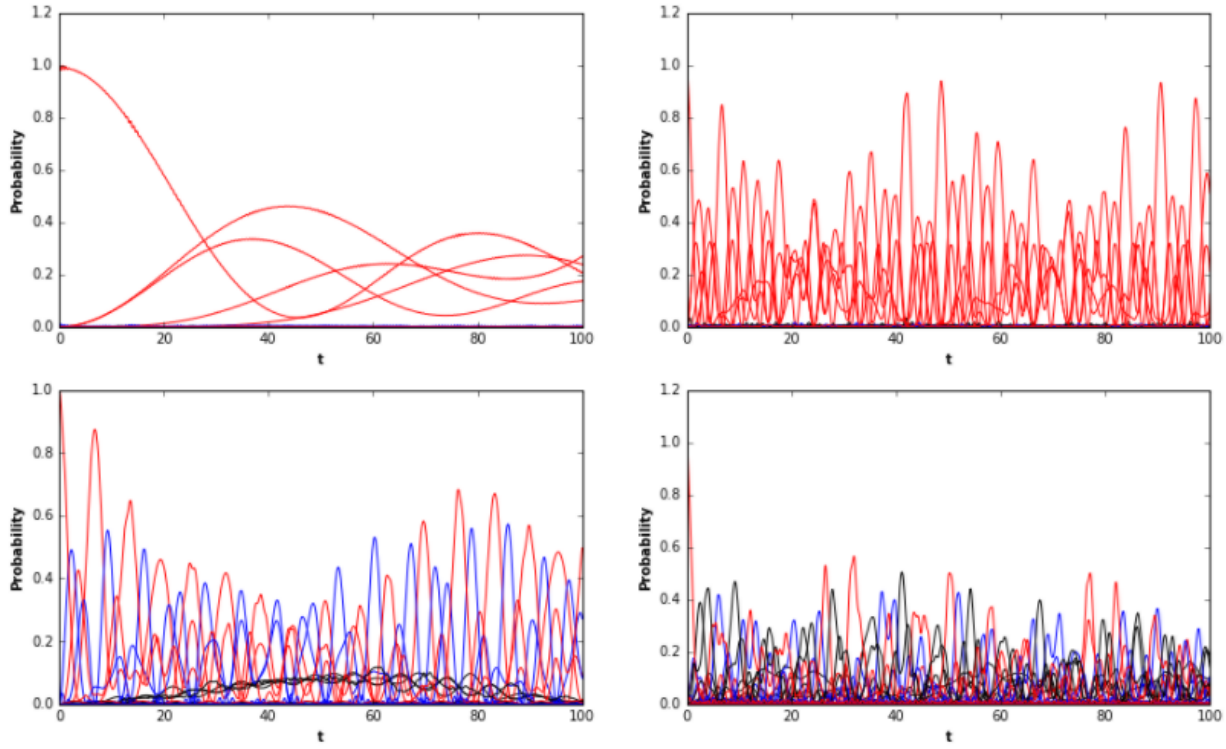

FIG. 8: Probabilities of all basis vectors for just NN interactions (top left), addition of NNN flip-flop coupling (top right), addition of NNN Ising interaction (bottom left), and addition of both Ising and flip-flop coupling (bottom right). Vectors with doublons are in red, vectors with the excitations as next nearest neighbors are in blue, and all other vectors are in black. The system has 8 sites, $\Delta = 10$, $\lambda = 1$, open boundary conditions, and the initial state is $|00001100\rangle$.

flip-flop coupling is extended to NNN sites (figure 8 top right panel), the same vectors show up in the dynamics, but the evolution is sped up. This is because the flip-flop term does not affect the diagonal terms in the Hamiltonian. The energy difference between basis vectors remains the same, but each basis vector is able to evolve into more vectors, speeding up the dynamics.

When the Ising interaction is extended to NNN sites (figure 8 bottom left panel), there are two effects. The first is that vectors with excitations on NNN sites behave like doublons. This makes sense because the NNN Ising interaction makes the diagonal terms corresponding to basis vectors with excitations on NNN sites be the same as the diagonal terms corresponding to basis vectors with doublons. The second effect is that the dynamics are sped up, like when the flip-flop coupling is extended. When there is only nearest neighbor interaction, to get from one doublon to another the system has to go through an intermediate non-doublon state. However, when the states with excitations as NNNs become effectively like doublons, the flip-flop term can immediately couple a doublon on neighboring sites to a doublon on NNN sites, so the system can evolve faster.

Some non-doublons also show up in the dynamics, but those turned out to all be vectors with an excitation on the border. Nevertheless, the fact that these border states show up shows that the speed of evolution of the system is significantly increased. In the final case where both the Ising and flip-flop interactions are extended (figure 8 bottom right panel), the dynamics are sped up to the point where border states seem to appears as much as doublons.

Even though these border states have different energy than the doublons, the combination of the border effect with the sped up dynamics ends up breaking the doublons on the boundary. The border states were not of concern in the case of nearest neighbor interactions because the

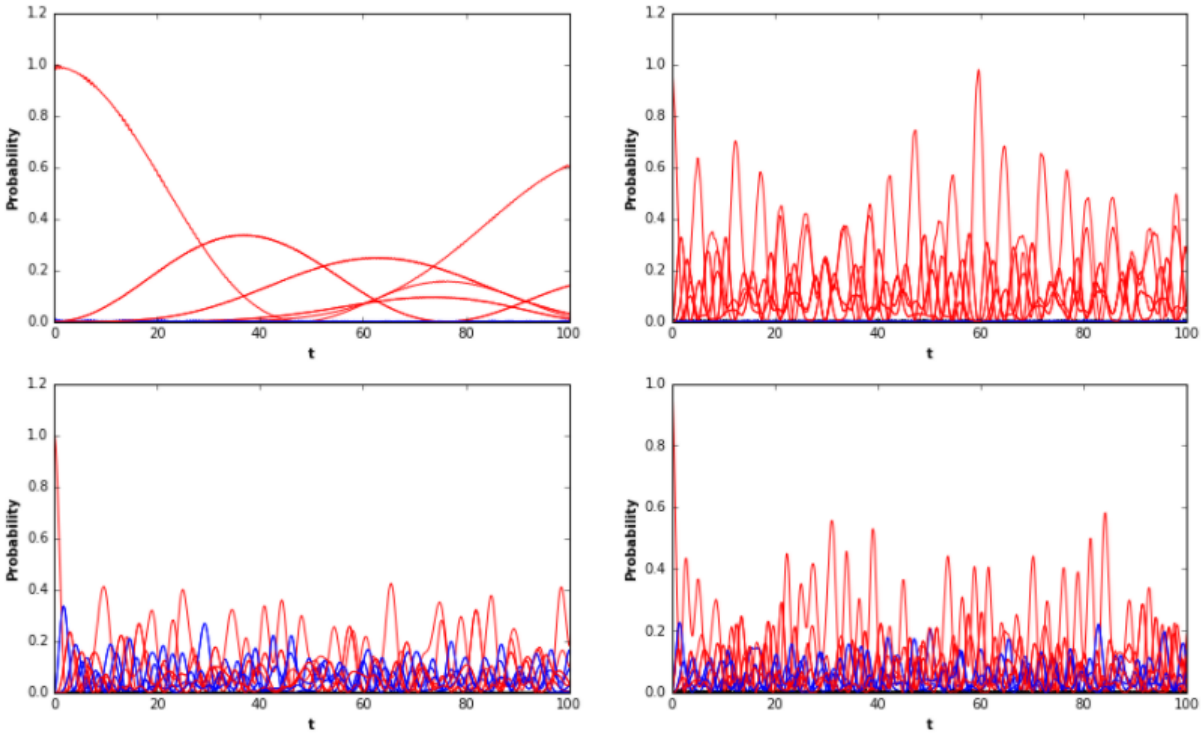

FIG. 9: Same as figure 8 but with closed boundary conditions.

dynamics were much slower, so we could use open boundary conditions without concern. However, we see that this is no longer true when NNN couplings are added, which suggests that using closed boundary conditions when dealing with systems with NNN couplings significantly simplifies the analysis.

Figure 9 shows the same cases with closed boundary conditions. In this case, the vectors with excitations on NNN sites become like doublons when the Ising interaction is extended, but no border states appear.

V. SYSTEMS WITH MANY EXCITATIONS

A. Integrable and Chaotic Systems

We will next discuss systems where the number of spins-up equals the number of spins-down. In this case, signatures of quantum chaos may become evident. To understand what this means, we must talk about what chaos is.

In classical mechanics, motion is characterized into two types: integrable and chaotic. Integrable motion is associated with linear differential equations for which exact analytical solutions can typically be found. Systems undergoing integrable motion either settle down to a steady state or an oscillation that is either periodic or quasiperiodic [13]. Because of the existence of analytical solutions and regular motion, the long term behavior of these systems can be predicted. Chaotic systems, on the other hand, are typically described by nonlinear equations and it is impossible to find analytical solutions for them. These systems exhibit extreme sensitivity to initial conditions, as described by positive Lyapunov exponents, and it is therefore impossible to predict their long term behavior [13]. Chaotic systems may also become ergodic, meaning that after a sufficiently

long time the system will visit an entire surface of constant energy in phase space.

In quantum mechanics, the same notions of integrable and chaotic cannot exist, as quantum mechanics is inherently linear due to the linearity of the Schrödinger equations. Additionally, the notion of phase space is meaningless in quantum mechanics because of superposition and the uncertainty principle, which states that we cannot know the precise position and momentum of a quantum particle at the same time. Nonetheless, quantum systems can still be characterized as integrable and chaotic. The quantum mechanical equivalents of classical integrable systems can be solved analytically, and their energy eigenvalues are uncorrelated and are allowed to cross. Conversely, the quantum mechanical equivalents of classical chaotic systems cannot be solved analytically and the spectrum of eigenvalues shows level repulsion. The eigenvectors of chaotic models are delocalized, meaning that they have significant contributions from many states. These signatures of quantum chaos can be used to extend the notion of quantum chaos to systems that do not have classical analogues [14].

In this section, we will be looking at three models, one integrable and two chaotic. The integrable model is the Heisenberg XXZ model from the previous section, with the addition of a small defect on the first site to break symmetries. As long as the defect is on the first site, the model is still integrable [15]. The Hamiltonian for the XXZ model is given by:

$$H = H_{XXZ} + \epsilon_1 J S_1^z \tag{26}$$

ϵ_1 is the magnitude of the defect on the first site, which I set to .1 in my codes.

For the second model, we add a defect of similar magnitude to J in the middle of the chain. We call this model the defect model. The Hamiltonian for this model is given by:

$$H = H_{XXZ} + dJ S_{N/2}^z + \epsilon_1 J S_1^z \tag{27}$$

where d is the magnitude of the defect. The presence of the defect makes the model chaotic, as long as the defect is not too small or too large. If the defect is very small relative to J, then its presence does not have a significant impact. If the magnitude of the defect is very large relative to J, then it merely breaks the system into two smaller chains. I used $d = .9$ in my codes.

Adding a defect is not the only way to make the Heisenberg model chaotic. In the third model, we add next nearest neighbor (NNN) couplings, which makes the model chaotic. We refer to this model as the NNN model, and its Hamiltonian is given by:

$$H = H_{XXZ} + \lambda H_{NNN} + \epsilon_1 J S_1^z \tag{28}$$

where λ is the strength of the NNN couplings.

Just as with the defect model, if the values of λ is too small then the NNN couplings will not have any significant impact on the system. If λ is too large, then the system will effectively be broken into two smaller chains. I set $\lambda = 1$ in my codes.

All three models conserve the number of excitations. We use system size $N = 16$, so the dimension is:

$$\mathcal{D} = \binom{16}{8} = \frac{16!}{(8!)^2} = 12870 \tag{29}$$

We do not have enough memory to handle larger systems.

B. Random Matrices

Even for integrable systems, attaining analytical results for some physical observables of these quantum systems with many and strongly interacting particles is extremely complicated and often

impossible. One way to get insight into this problem is to use random matrices. Instead of using a Hamiltonian that models a realistic system, we use a matrix filled with random numbers. Random matrices were first used by Eugene Wigner to model the spectra of heavy nuclei, and they have since been applied to a variety of complex physical systems, including atoms, molecules, and quantum dots [14]

In the approach of using full random matrices for the Hamiltonian, interactions are treated statistically and the details are overlooked. The matrices are only constrained to satisfy the symmetries of the system [16]. We use the Gaussian Orthogonal Ensemble (GOE) of full random matrices, which is used to model systems with time reversal symmetry. GOE full random matrices are $\mathcal{D} \times \mathcal{D}$ real and symmetric matrices with entries from a Gaussian distribution with mean 0. The diagonal elements have variance 2 and the off-diagonal elements have variance 1. A GOE full random matrix can be obtained by generating a $\mathcal{D} \times \mathcal{D}$ matrix with entries from a standard normal distribution and adding it to its transpose [17]. These matrices are not realistic because they imply that all particles interact at the same time. Additionally, they imply that faraway interactions are as strong as nearby interactions.

C. Static Properties

Just as for systems with two excitations, we start by looking at the eigenvalues and eigenstates of the Hamiltonians.

1. Eigenvalues: Density of States

We start by looking at the eigenvalues of the Hamiltonians. One quantity of interest is the density of states, which is basically a histogram of the eigenvalues. Wigner first derived that the density of states of GOE random matrices follows a semicircle distribution [16], given by:

$$\rho(E) = \frac{2}{\pi \mathcal{E}} \sqrt{1 - \left(\frac{E}{\mathcal{E}}\right)^2} \tag{30}$$

where the eigenvalues range from $-\mathcal{E}$ to $\mathcal{E}$.

Figure 10 shows the numerically obtained density of states for the random matrix and for the three realistic models. The semicircle distribution for the random matrix agrees with the analytical result. The three realistic models, whether integrable or chaotic, all have Gaussian densities of states. It turns out that the Gaussian density of states is general for all systems with just two body interactions as the number of spins-up approaches the number of spins-down. This is one way in which GOE random matrices differ from realistic systems.

2. Eigenvalues: Unfolding

When we study the spectra of eigenvalues of quantum systems, we are interested in the fluctuations of the energy levels. However, we cannot compare the energy level spacings of different systems with different average spacings, or even different regions of the spectrum of one system with different average spacings. Therefore, we must rescale the eigenvalues so that the local mean level spacing is 1. The process of rescaling the energy levels is called unfolding, and there are many ways to do it. I will first describe a simple unfolding procedure and then a more sophisticated procedure given in [14].

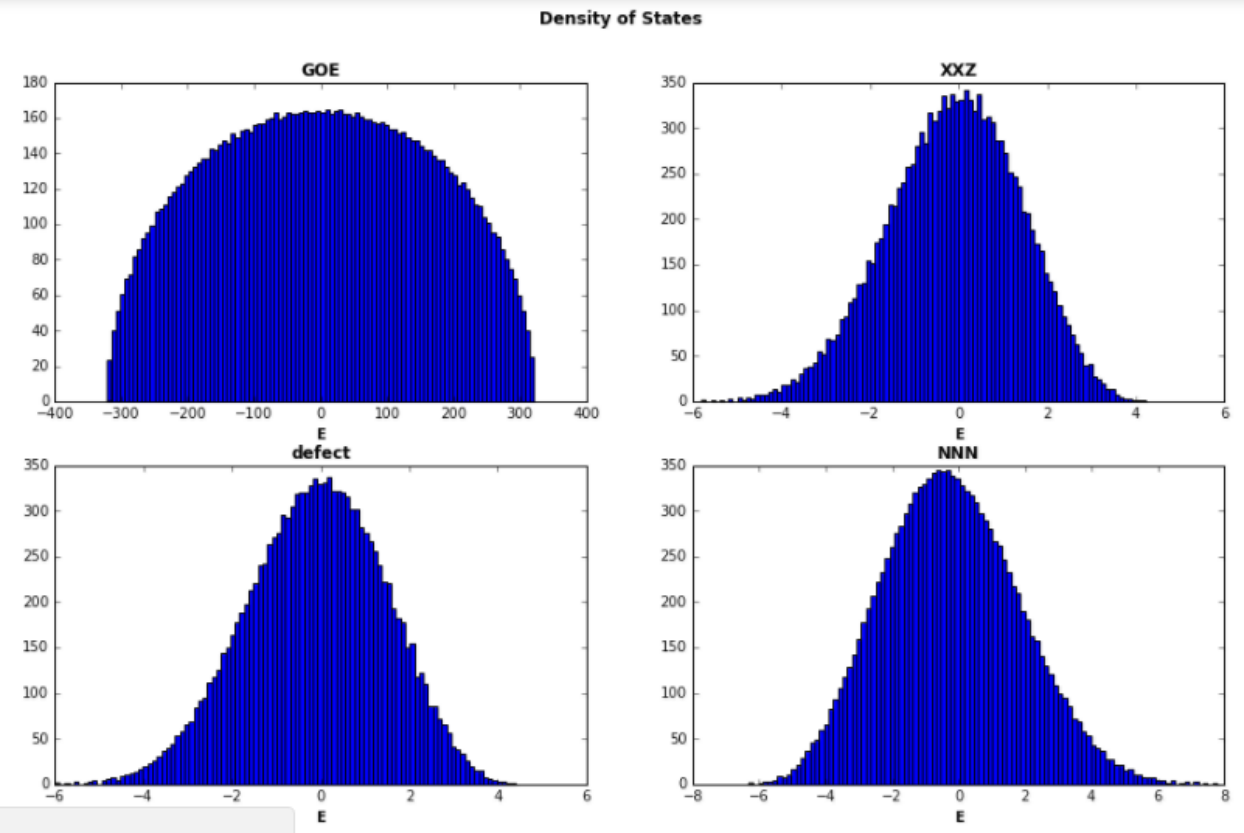

FIG. 10: Density of States for GOE random matrices and the three realistic models.

The first step in the simple unfolding procedure is to order then eigenvalues in order of increasing energy, which NumPy already does for you. Next, discard a certain percentage of the eigenvalues from the edge of the spectrum, where the fluctuations are large. Obtain an array of spacings between neighboring eigenvalues. Split the spacings into small groups, say of size 10. Divide each group by its average, and then the mean level spacing is 1.

This simple approach works for some purposes, but it has some problems. The average spacing at the border between groups is not 1, which affects the calculation of the long range fluctuations in the spectrum.

The more sophisticated approach also starts out by ordering the eigenvalues by increasing energy and cutting a specific percentage of eigenvalues off of each end. The next step is to obtain the cumulative spectral function, given by:

$$\eta(E) = \sum_{n=1}^{N} \Theta(E - E_n) \tag{31}$$

where N is the number of eigenvalues left after cutting some off of each end and Θ is the Heaviside function, given by:

$$\Theta(x) = \begin{cases} 0, & x < 0 \\ 1, & x \geq 0 \end{cases} \tag{32}$$

In practice, the cumulative spectral function simply counts the number of eigenvalues less than a given energy. The function is also known as the staircase function because it has a staircase-like

structure. The function can be separated into a smooth part $\xi(E)$ and a fluctuating part $\eta_{fl}(E)$, and is then given by:

$$\eta(E) = \xi(E) + \eta_{fl}(E) \tag{33}$$

The smooth part can be obtained by fitting a polynomial to the cumulative spectral function. We choose to use a polynomial of degree 15. Finally, the unfolded eigenvalues are given by the function ξ acting on the original eigenvalues.

Codes for both unfolding procedures are given in the appendix.

3. Eigenvalues: Level Spacing

A hallmark of quantum chaos is that the eigenvalues of a chaotic system are rigid and show level repulsion. Integrable systems, on the other hand, can have uncorrelated eigenvalues that are allowed to cross. Level repulsion can be detected by looking at the distribution of spacings between neighboring energy levels of the unfolded eigenvalues. The distribution of spacings is known as the level spacing distribution and is denoted $P(s)$, where s is the spacing between neighboring levels. For GOE full random matrices, level spacing is given by the Wigner-Dyson distribution [16]:

$$P(s) = \frac{\pi s}{2} \exp\Big(- \frac{\pi s^2}{4} \Big) \tag{34}$$

For uncorrelated eigenvalues, where there is no level repulsion, the level spacing distribution is Poisson, given by:

$$P(s) = \exp(-s) \tag{35}$$

Figure 11 shows the level spacing distributions for a GOE random matrix and the three realistic models. The spacings for random matrix and chaotic models have Wigner-Dyson distributions, while the spacings for the integrable XXZ model follows a Poisson distribution.

4. Eigenvalues: Level Number Variance

From the level spacing distributions alone, it looks like the spectra of the defect and NNN models have the same rigidity as that of the GOE full random matrix. However, we find differences when we look at another measure of rigidity of the spectrum, the level number variance. Level number variance, denoted $\Sigma^2(\ell)$, is the variance of the number of unfolded eigenvalues in an interval of length ℓ.

Level spacing and level number variance are complementary quantities. Level spacing measures the short range fluctuations of the spectrum while level number variance measures the long-range fluctuations. It is therefore useful to look at both quantities together.

For uncorrelated eigenvalues, the level number variance is linear: $\Sigma^2(\ell) = \ell$, and the completely rigid spectrum of the harmonic oscillator has $\Sigma^2(\ell) = 0$. For the GOE random matrix, the level number variance is given by [14]:

$$\Sigma^2(\ell) = \frac{2}{\pi^2}\Big(\ln(2\pi\ell) + \gamma_e + 1 - \frac{\pi^2}{8} \Big) \tag{36}$$

where $\gamma_e = .5722...$ is the Euler gamma constant. The logarithmic behavior of the level number variance for GOE full random matrices is between the linear dependence for uncorrelated eigenvalues and 0 for the completely rigid harmonic oscillator.

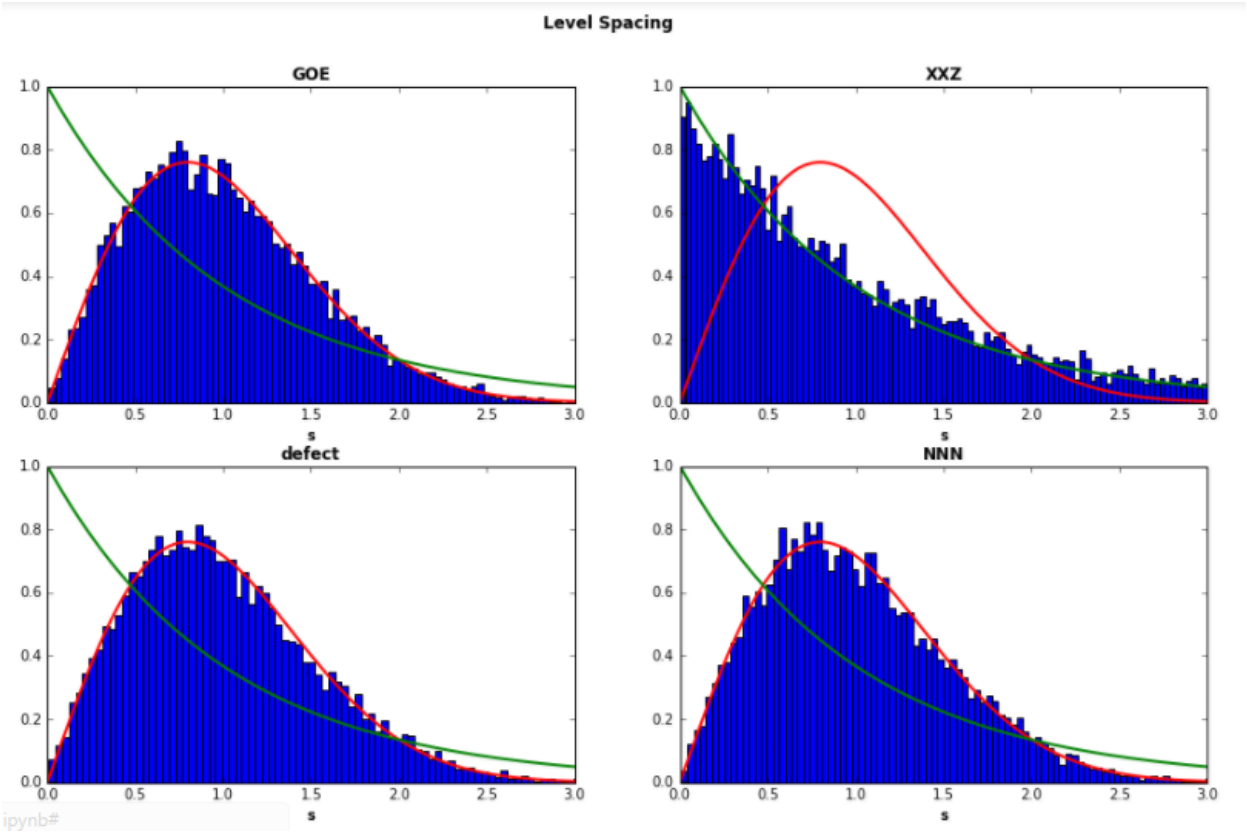

FIG. 11: Level spacing distributions for the four models under consideration. The analytical curve for the Wigner-Dyson distribution is shown in red, and the curve for the Possion distribution is shown in green.

Figure 12 shows the level number variance for the GOE full random matrix and the three realistic models. The numerical data for the random matrix agrees well with the logarithmic analytical expression. The numerical result for the integrable XXZ model follows the linear curve for low values of ℓ but does not follow it perfectly for higher values of ℓ because of the finite system size. The data for the two chaotic models starts out logarithmic but then increases at a greater rate than the logarithmic expression. This shows that the spectra for the realistic chaotic models is not as rigid as that of the GOE full random matrix, and it shows the importance of using different signatures of quantum chaos when comparing models.

5. Eigenvectors: Delocalization

After analyzing the properties of the eigenvalues, we move on to the eigenvectors. We are interested in measuring the level of delocalization, or spread, of the eigenvectors in a particular basis. As we saw before, delocalization can be measured by using the participation ratio (PR). The notion of basis is not well defined, but we can still give values to the measures of delocalization. The eigenvectors of the GOE random matrix are themselves random vectors from a Gaussian distribution, and they remain random vectors under any change of basis. Since the eigenvectors are random vectors, all eigenstates are roughly equivalent and have approximately the same PR of about $\mathcal{D}/3$.

A similar quantity that is often used to measure delocalization is the Shannon information entropy. Given an eigenvector $|\psi\rangle = \sum_k C_k |\phi_k\rangle$ written in a certain basis $|\phi_k\rangle$, the Shannon

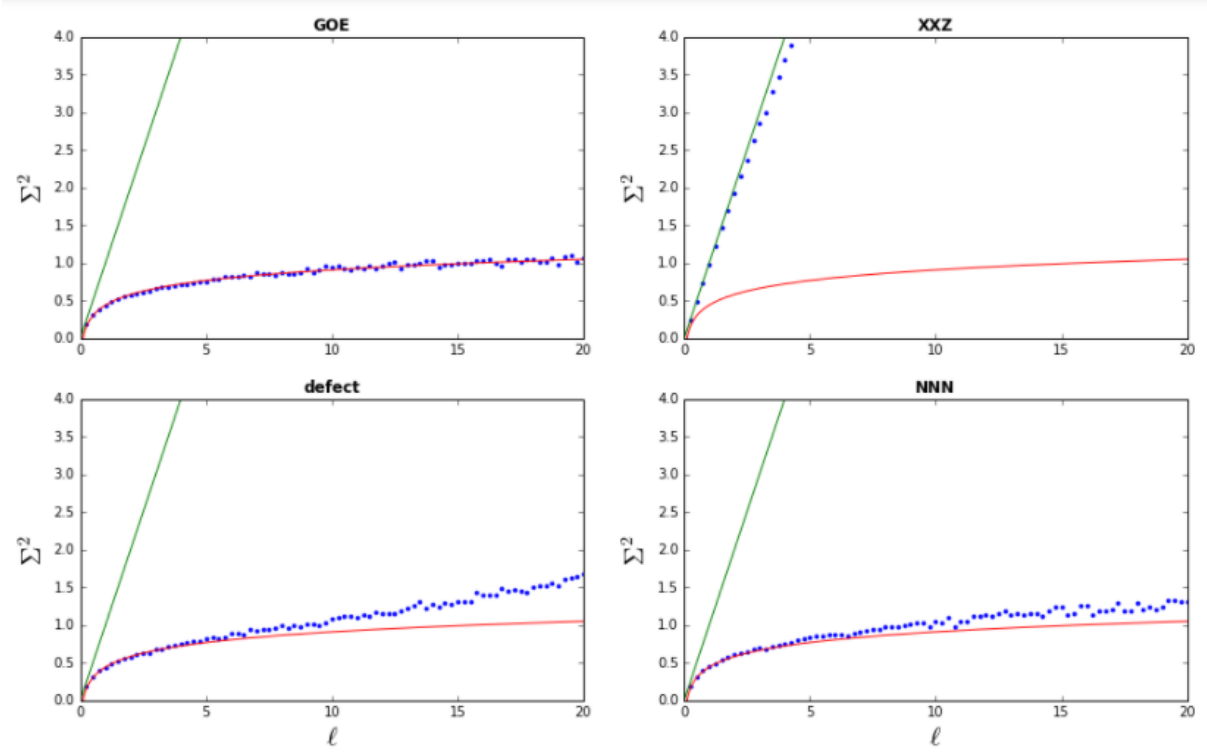

FIG. 12: Level number variance for a GOE random matrix and the three realistic models. Numerical data is in blue, the analytical curve for the logarithmic expression is given in red, and the linear curve is given in green.

entropy of the eigenvector is given by:

$$S_{sh} = -\sum_{k=1}^{\mathcal{D}} |C_k|^2 \ln |C_k|^2 \tag{37}$$

A Python code for finding the Shannon entropy of eigenvectors is given in the appendix.

In order to obtain an analytical result for the Shannon entropy of the GOE random matrix, we must approximate the sum as an integral. Since the probability distributions $P(C_k)$ are all identical, we can approximate the sum of a function $f(C_k)$ by its expectation value, giving:

$$\sum_{k=1}^{\mathcal{D}} f(C_k) \approx \mathcal{D} \int_{-\infty}^{\infty} f(C) P(C) dC \tag{38}$$

In this case, the probability distribution is Gaussian and is given by:

$$P(C) = \sqrt{\frac{\mathcal{D}}{2\pi}} \exp\left(\frac{-\mathcal{D}C^2}{2}\right) \tag{39}$$

and $f(C) = C^2 \ln(C^2)$. The Shannon entropy can then be approximated as:

$$S_{sh} \approx -\mathcal{D}\sqrt{\frac{\mathcal{D}}{2\pi}} \int_{-\infty}^{\infty} C^2 \ln(C^2) \exp\left(\frac{-\mathcal{D}C^2}{2}\right) dC = -2 + \ln(2) + \gamma_e + \ln(\mathcal{D}) \approx \ln(.48\mathcal{D}) \tag{40}$$

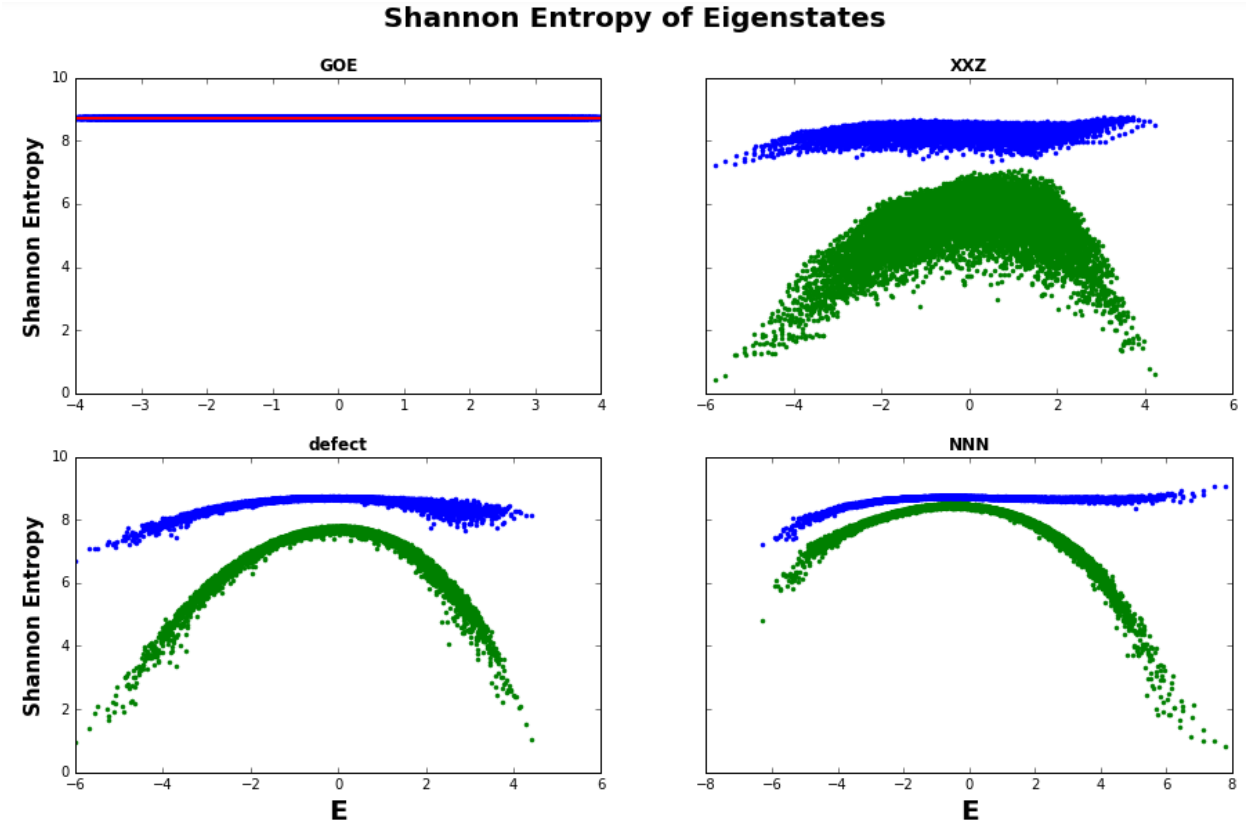

FIG. 13: Shannon Entropy for the GOE random matrix and the three realistic models. For the GOE random matrix, the Shannon entropy is given in blue and the analytical expression is given in red. For the three realistic models, the Shannon entropy in the site basis is given in blue, and the Shannon entropy in the mean field basis is given in green.

For the three realistic models, the result for the Shannon entropy depends on the basis chosen. Which basis we choose depends on what we are interested in measuring. If we are interested in delocalization in real space, then we use the site basis. If we are interested is in the level of chaoticity of the eigenstates, then we use the so called mean field basis. The mean field basis is the basis of eigenvectors of the integrable part of the Hamiltonian. For the defect and NNN models, we use the eigenstates of the XXZ model as the mean field basis. For the XXZ model, we use the eigenvectors of the XX model, that is the XXZ model without Ising interactions.

Figure 13 shows the results for Shannon Entropy. The numerical results for the GOE random matrix do not fluctuate much and agree very well with the analytical expression. For the realistic models, we see that the results for the mean field basis differ greatly from the results in the site basis, highlighting how much Shannon entropy is basis dependent. In both bases, we see greater fluctuation for the integrable XXZ model than for the two chaotic models. Likewise, in the mean field basis, the Shannon entropy of the XXZ model is smaller overall than for the two chaotic models. This is because the eigenstates of the integrable XXZ model are further from random vectors than the eigenstates of the chaotic models. In the mean field basis, the Shannon entropy for the two chaotic models approaches the value of that of the random matrices, indicating that they are more delocalized and chaotic in the middle of the spectrum. At the edges of the spectrum, the Shannon entropy decreases, which shows that the states at the end of the spectrum are more localized.

6. Eigenvectors: Entanglement Entropy

Say that we split our system of 16 sites into two halves: A and B, and we want to measure the spins on the 8 sites of A. We cannot look at subsystem A alone, as the sites in A are affected by the sites in B. We therefore say that system A and system B are entangled. We can measure the amount of entanglement in a state by using the Von Neumann Entanglement Entropy, but first we must introduce concept of the density matrix.

Until now, we have been considering systems whose quantum states can be completely described by a single vector Ψ. In this case, even though the result of measurement on the system is probabilistic, the state vector that represents the system is deterministic. We know the initial vector that represents the system and this state evolves deterministically as described by the Schrödinger equation. However, this all assumes that we are sure about the initial state of a system. Consider, by contrast, a case where we study ensembles of systems. In that case, we can assume that we attempt to prepare the system in the same initial state many times. However, we cannot always be sure that we always prepare the same initial state. Therefore, our information on the state of the system is not complete, and we cannot represent the state of a system by a single vector.

In order to represent our system, assume that the system has probability w_k to be found in the state $|\Psi_k\rangle$. We then define the density operator ρ by:

$$\rho = \sum_k w_k \left|\Psi_k\right\rangle \left\langle\Psi_k\right| \tag{41}$$

The density operator is the sum of the projection operators for each state weighted by the probability of the system being in that state. In the case where there is only one state, it is referred to as a pure state. When there are multiple possible states, it is referred to as a mixed state, and it is impossible to write the density matrix as the projection operator associated with a single state [18]. In our case, the systems are finite, so the density operators are matrices. Additionally, we are dealing with pure states, so the density matrix of each eigenstate is the outer product of the eigenvector with itself.

In order to find the entanglement entropy of an eigenvector, we first find the density matrix ρ associated with that eigenvector. We then split the system into two halves, A and B, and take the partial trace of the density matrix with respect to the sites in B. The result is the reduced density matrix in A, given by:

$$\rho_A = Tr_B(\rho) \tag{42}$$

where ρ_A is the reduced density matrix associated with A and Tr_B is the partial trace with respect to B. Since the system is entangled, the reduced density matrix represents a mixed state.

Finally, the entanglement entropy can be found from the reduced density matrix, by:

$$S_{vN} = -Tr(\rho_A \ln \rho_A) \tag{43}$$

A code for finding the Von Neumann Entanglement Entropy of a complex state is given in the appendix.

Figure 14 shows the Entanglement Entropy for a GOE full random matrix and the three realistic models. For the random matrix, the result is constant, just like the Shannon Entropy. For the realistic models, the results seem to convey the same information as the Shannon Entropy in the mean field basis. Just as for the Shannon entropy in the mean field basis, the Entanglement Entropy of the XXZ model fluctuates more and is overall lower than for the chaotic models. Likewise, the

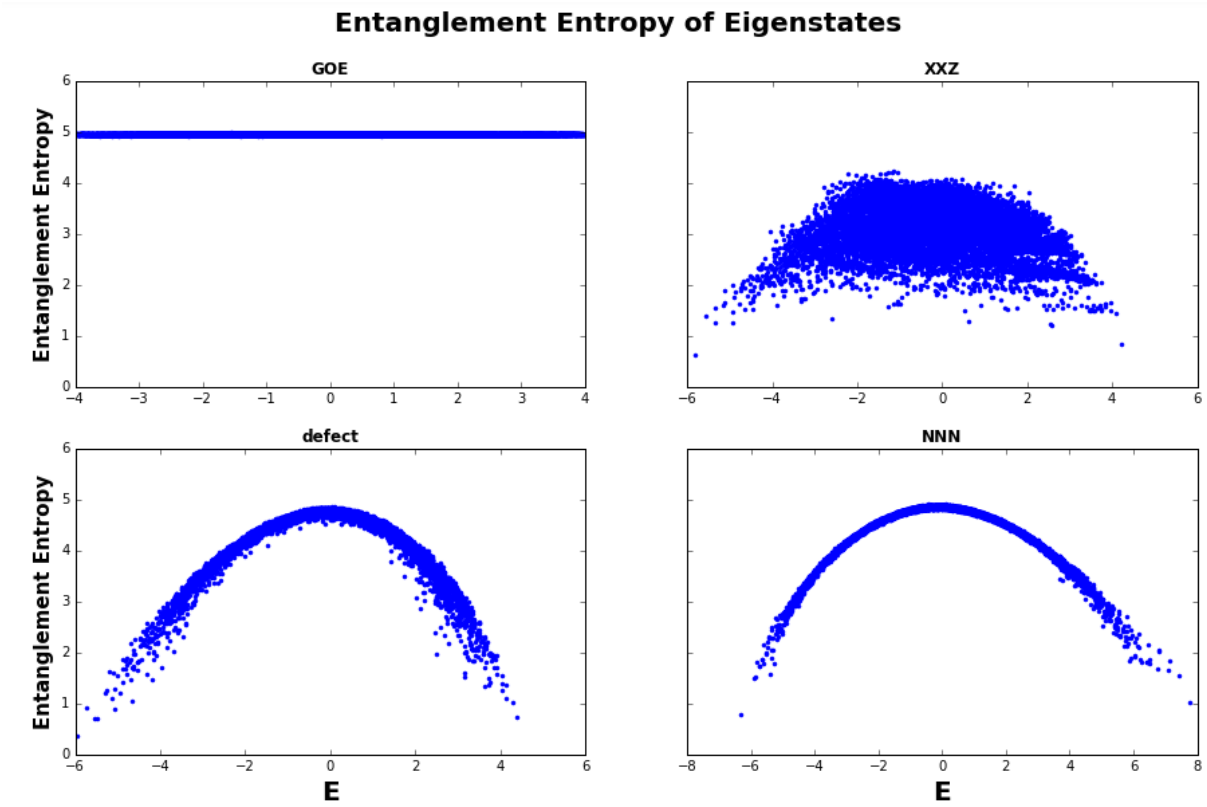

FIG. 14: Von Neumann Entanglement Entropy of the eigenvectors for the GOE full random matrix and three realistic models.

chaotic models have Entanglement Entropy close to that of the random matrix in the center of the spectrum but it decreases closer to the border.

The fact that both entropies seem to convey the same information is important. The Von Neumann Entanglement Entropy is often used to measure the complexity of the eigenstates of quantum systems. However, calculating the Entanglement Entropy is computationally more expensive, and it took days for a computer to calculate for the systems we studied. The Shannon Entropy, by contrast, takes significantly less time to calculate. Moreover, Shannon Entropy is experimentally accessible, while the Entanglement Entropy would be much more involved to measure. It therefore seems that the Shannon Entropy is a more practical measurement of the level of complexity of eigenstates. Although, Shannon Entropy has the drawback that it is dependent on the basis chosen, while that does not matter for Entanglement Entropy.

D. Dynamic Properties

We now move to describe the dynamics for our models. In the following sections, we use the initial state $|\downarrow\uparrow\downarrow\uparrow ...\rangle$. This is known as the Néel state, and it is often prepared in experiments involving ultracold atoms. Although, these experiments are often done with boson particles, so instead of 1 and 0 representing spin-up and spin-down, they can represent a site that is or is not populated. For the GOE random matrix, we use the row in the middle of the matrix of eigenvectors as the initial state.

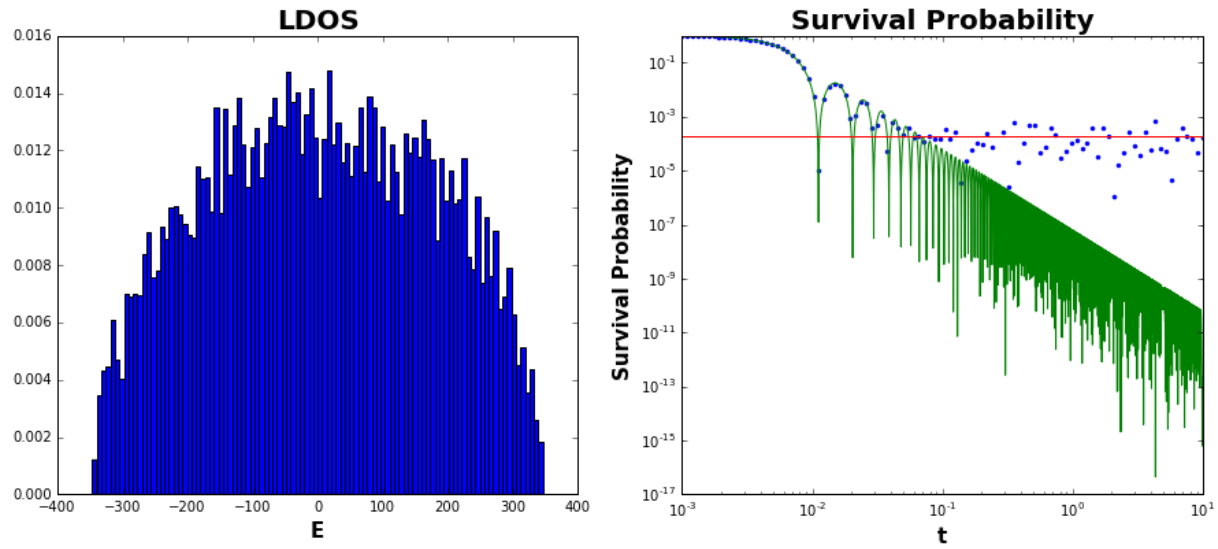

FIG. 15: Local density of states (left) and survival probability (right) for a GOE full random matrix. The numerical results for survival probability are in blue, the analytical result is in green, and the saturation value is given in red.

1. *Survival Probability*

Just as in the section on doublons, we characterize the speed of the dynamics by looking at the decay of the survival probability. Let us define the quantity:

$$P_{ini,ini}(E) = \sum_{\alpha=1}^{\mathcal{D}} |C_{ini}^{\alpha}|^2 \delta(E - E_\alpha) \tag{44}$$

This is the energy distribution of the initial state weighted by the probabilities of each eigenvector in the initial state. It is often referred to as the local density of states (LDOS). The survival probability can be written as:

$$W_{ini}(t) = \left| \int_{-\infty}^{\infty} P_{ini,ini}(E) dE \right|^2 \tag{45}$$

The survival probability can then be found by taking the fourier transform of the LDOS.

Figure 15 shows that the LDOS for a GOE full random matrix is given by a semicircle distribution with some fluctuations, which is analogous to its density of states. Taking the Fourier transform of a semicircle, we end up with the analytical result:

$$W_{ini}(t) = \frac{[\mathcal{J}_1(2\sigma_{ini}t)]^2}{\sigma_{ini}^2 t^2} \tag{46}$$

where $\mathcal{J}_1$ is the Bessel function of the first kind,

$$\sigma_{ini}^2 = \langle \Psi(0) \,|\, H^2 \,|\, \Psi(0) \rangle - \langle \Psi(0) \,|\, H \,|\, \Psi(0) \rangle^2 = \sum_{\alpha=1}^{\mathcal{D}} |C_{ini}^{\alpha}|^2 (E_\alpha - E_{ini})^2 \tag{47}$$

is the variance of the energy distribution of the initial state, and

$$E_{ini} = \langle \Psi(0) \,|\, H \,|\, \Psi(0) \rangle = \sum_{\alpha=1}^{\mathcal{D}} |C_{ini}^{\alpha}|^2 E_\alpha \tag{48}$$

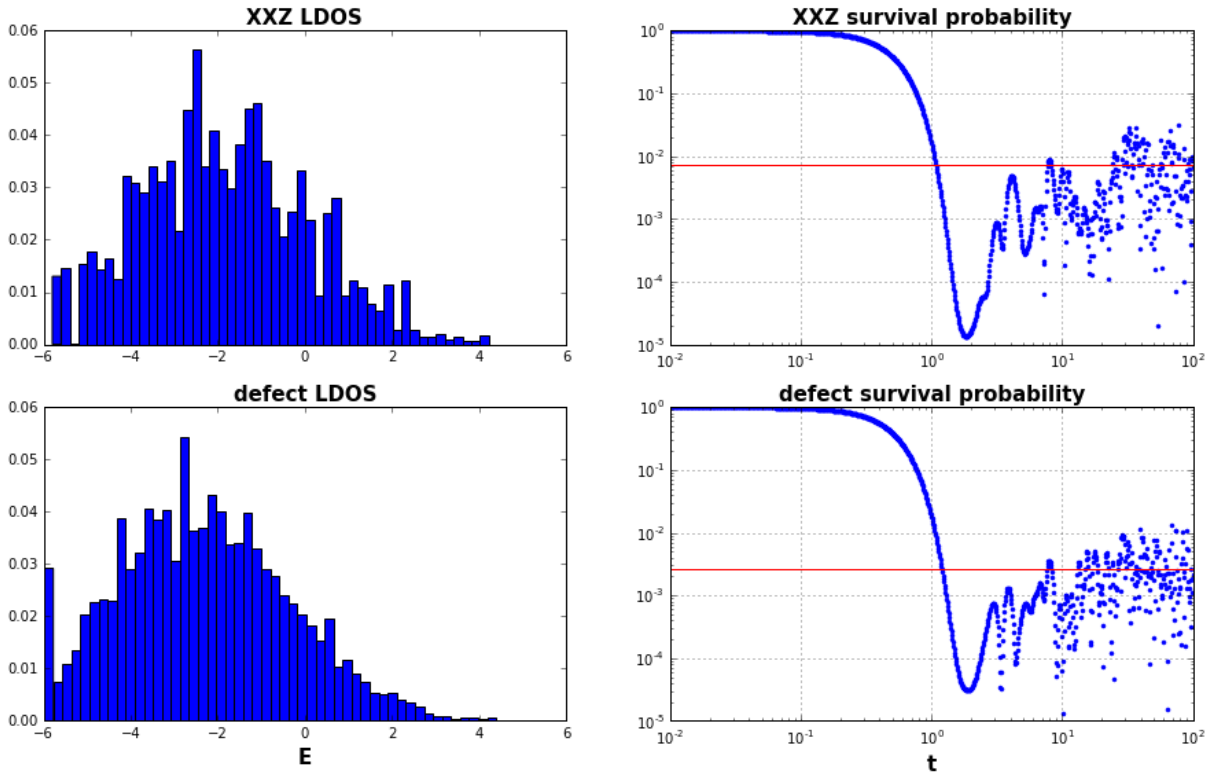

FIG. 16: LDOS and survival probability for the XXZ and defect models. For the survival probability, the numerical data is given in blue and the saturation value is given in red.

is the energy of the initial state.

Figure 15 on the right shows the numerical and analytical results for the survival probability for the GOE full random matrix. The numerical data fits the analytical expression very well at first, but then it starts to saturate because of the finite system size. The very wide LDOS shows that the system is very far from equilibrium, so the system evolves extremely quickly.

The value at which the survival probability saturates can be found by expressing the survival probability as:

$$W_{ini} = \sum_{\alpha=1}^{\mathcal{D}} |C_{ini}^{\alpha}|^4 + \sum_{\alpha \neq \beta} |C_{ini}^{\alpha}|^2 |C_{ini}^{\beta}|^2 e^{i(E_\beta - E_\alpha)t} \tag{49}$$

After some time, the oscillating term cancels itself out, leaving just the first term.

Figure 16 shows the LDOS and survival probability for the XXZ and defect models. In both cases, the LDOS is a Gaussian with fluctuations, which shows the initial state is spread out in the basis of eigenvectors, but not as much as the initial state is spread out for the GOE full random matrix. Therefore, the survival probability decays very fast, but not as quickly as the survival probability for the random matrix. For both realistic models, the survival probability has a Gaussian decay [17], as expected, since the Fourier transform of a Gaussian is a Gaussian. This shows that quantum systems, even integrable quantum systems can have faster than exponential dynamics. These fast dynamics at intermediate time scales are generic for any realistic system taken abruptly far from equilibrium. It is only at longer time scales that there is a discernible difference between integrable and chaotic systems [19].

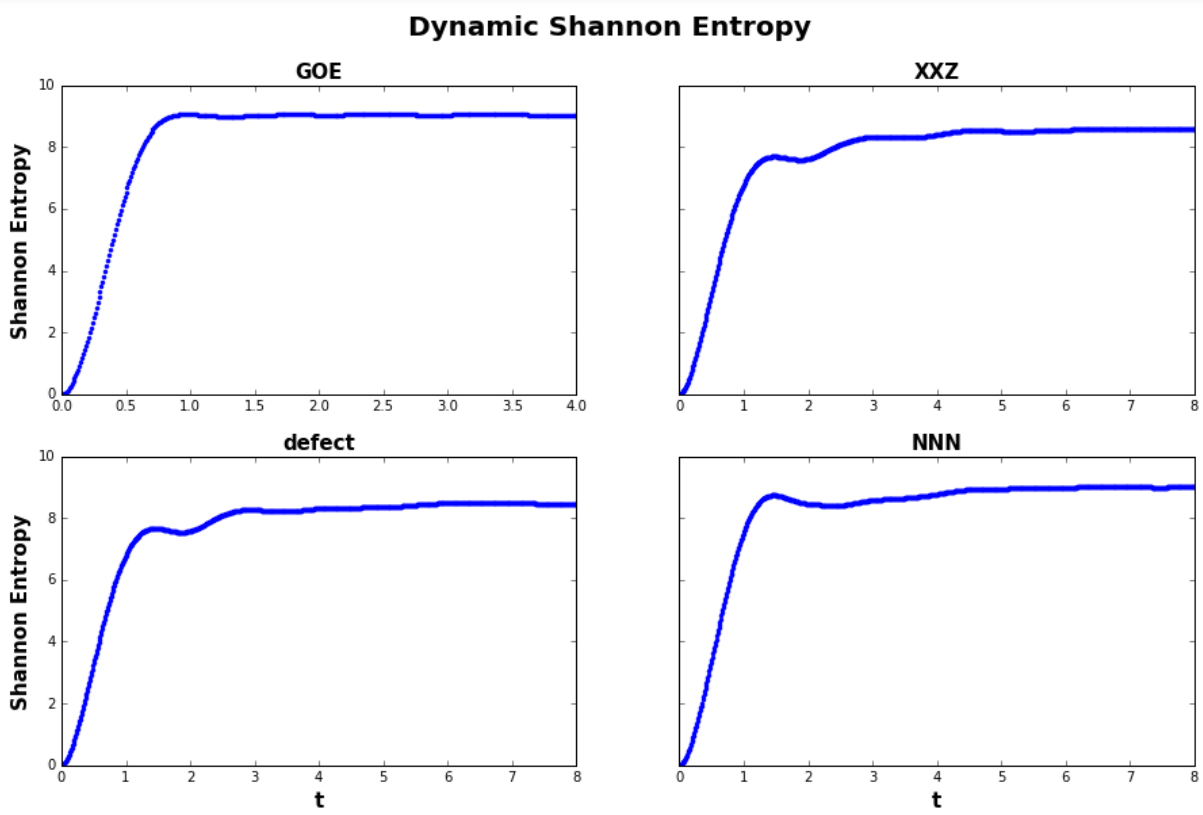

FIG. 17: Dynamic Shannon Information Entropy for the four models under consideration

2. *Evolution of Entropies*

We now look at the evolution of the Shannon and Entanglement entropies. That is, we study the Shannon and Entanglement entropies of the state of the system as a function of time. The evolution of the Shannon Entropy is given by:

$$S_{sh}(t) = -\sum_{k=1}^{\mathcal{D}} W_k(t) \ln W_k(t) \tag{50}$$

where $W_k(t)$ is the probability of measuring the basis vector $\phi(k)$ at time t. A code for finding the dynamic Shannon Entropy is given in the appendix. The dynamic Von Neumann Entropy can be found by solving for the wavefunction and then using the code for Entanglement Entropy given in the appendix.

Figures 17 and 18 show the dynamic Shannon and Entanglement entropies respectively. Both of them show a linear increase and then leveling off for all four models. The linear increase in the Shannon Entropy indicates an exponential spreading of the initial state, again showing the generic fast dynamics at intermediate time scales. Additionally, once again we seem to get the same information from the Shannon and Entanglement Entropies.

VI. CONTINUING RESEARCH: SYSTEMS WITH DISORDER

Any real system has disorder, where impurities cause different sites to have different energies. We represent disorder by using random numbers to represent the on site energies.

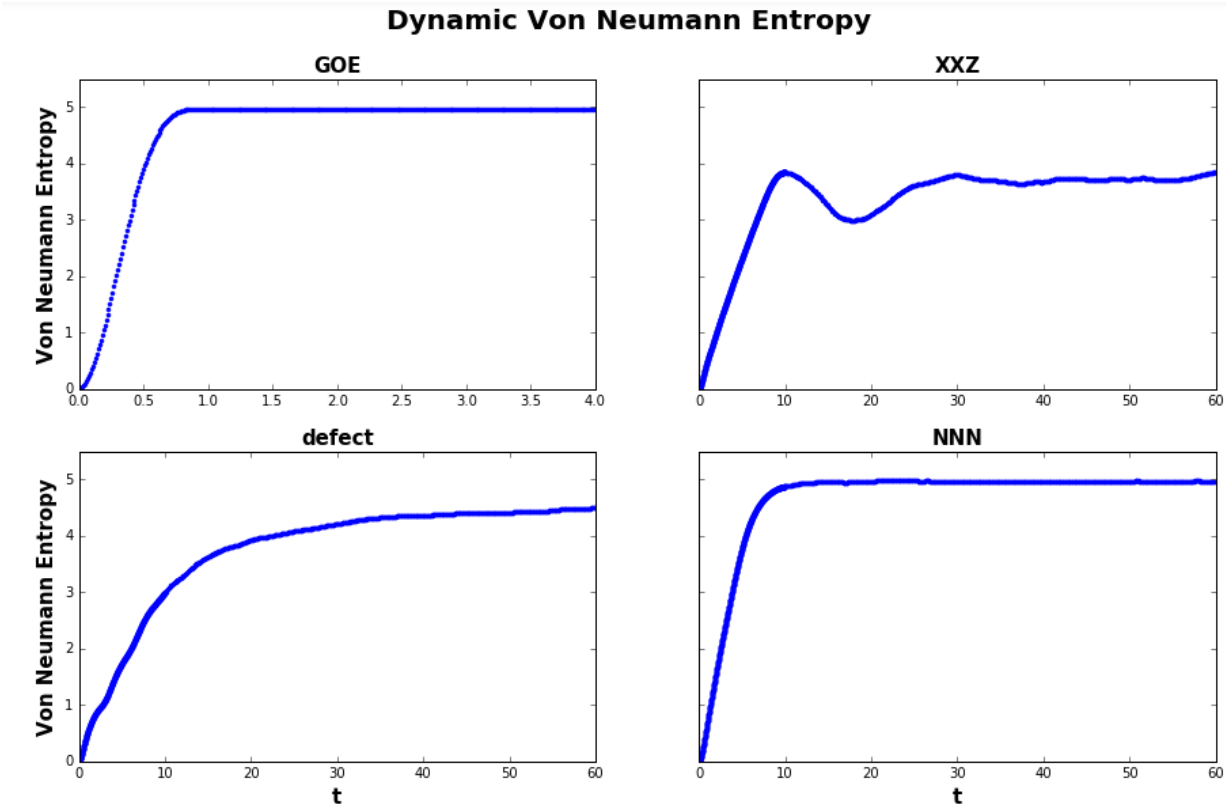

FIG. 18: Dynamic Von Neumann Entanglement Entropy for the four models under consideration

According to the Drude model of conductance, a metal conducts electricity because of free electrons that are allowed to move around the metal. If electrons are not able to move around the material freely, then it becomes an insulator. Philip Anderson studied systems of electrons in lattices using a model with disorder but without Ising interaction, and he showed that the electrons localize, meaning that they only have significant probabilities of being found in sites in a particular area, causing the system to be an insulator. Anderson found that in one dimension the electrons localize for any disorder magnitude, and in two dimensions the electrons localize when the disorder magnitude is above a critical value [20].

Subsequent studies of one dimensional models with interaction have shown that localization is still achieved with disorder above a certain critical value, like in the case of two dimensional non-interacting spins. We hope to establish a connection between two dimensional models without interaction to one dimensional models with interaction. We have been studying one dimensional models interactions and disorder modeled by random numbers. We have been representing observables such as the survival probability, Shannon Information Entropy, and Von Neumann Entanglement Entropy by taking averages over numerous random disorder realizations. We have to diagonalize a new Hamiltonian for each disorder realization, making all calculations computationally expensive and take a long time.

VII. CONCLUSION

We studied one-dimensional spin-1/2 systems with only two and with many excitations, analyzing how the static and dynamic properties of these systems depend on the parameters of the

Hamiltonian. Our results should appeal to the broad communities of experimentalists and theoreticians dedicated to the analysis of non-equilibrium many-body quantum dynamics, quantum speed limits, quantum chaos, many-body localization, and thermalization.

By studying simple one dimensional spin systems with two excitations, we have seen the nature of the two terms in the Heisenberg model Hamiltonian and the effect of changing the level of anisotropy, or ratio of the strengths of the Ising interaction and flip-flop interaction. We see that for high levels of anisotropy, two excitations stick together in a bound state that we call a doublon, which moves as one slow particle. When we add next nearest neighbor and longer-range interactions, the doublons split. We also see that whether we choose open or closed boundary conditions matters more when we add long-range interactions, speeding up the dynamics.

For systems with the number of excitations close to half of the number of spins, one dimensional systems can show strong signatures of quantum chaos. We compared one integrable model, two chaotic models, and GOE full random matrices. Random matrices do not represent realistic systems becuase they imply that all paticles interact at once and that faraway interactions are as strong as nearby interactions. Even so, random matrices are useful because their eigenvectors are themselves random vectors, allowing us to derive analytical results that fit well with the numerical data.

The density of states for a GOE random matrix follows a semicircle distribution, while realistic systems, whether integrable or chaotic, have Gaussian densities of states. This is because any system with only two body interactions approaches a Gaussian density of states when the number of excitations is large. This is one major difference between realistic Hamiltonians and random matrices.

When we look at the fluctuations of energy levels, we see that the results for chaotic models are closer to those for full random matrices. After performing the unfolding procedure, we find that the level spacing distribution for the integrable model is Poisson, while the distribution for the chaotic models and random matrices is Wigner-Dyson. The major difference is that the eigenvalues of an integrable model are uncorrelated and therefore allowed to cross. Conversely, chaotic models and full random matrices exhibit level repulsion, making the spectrum of energy levels rigid and preventing neighboring energy levels from crossing. Level repulsion is one of the main features of quantum chaos. When we look at the level number variance, another gauge of quantum chaos, we see that it is linear for the integrable model and logarithmic for the full random matrices. For the chaotic models, the level number variance is logarithmic at first, but then it increases faster than logarithmically, which shows that the spectrum for chaotic models is not as rigid as for full random matrices. This result also highlights the importance of using multiple signatures of quantum chaos in analyzing our models.

Since the eigenvectors of a GOE full random matrix are themselves random vectors, the Shannon Entropy in any basis is approximately constant for all eigenvectors. For realistic models, the Shannon Entropy is highly dependent on basis. We consider two bases, the site basis and the mean field basis. In both bases, we saw that for the integrable model the Shannon Entropy is lower overall and shows greater fluctuations than for the chaotic models. For the chaotic models in the mean field basis, in the middle of the spectrum the Shannon Entropy is close to the value for full random matrices, indicating that the eigenvectors corresponding to eigenvalues in the middle of the spectrum are close to random vectors.

We also saw that for both the eigenstates and the dynamics, the Shannon Entropy in the mean field basis seems to give the same information as the Von Neumann Entanglement Entropy. This is a significant result because the Von Neumann Entanglement Entropy is used extensively, yet it is computationally more expensive than the Shannon Entropy and it is much more difficult to measure experimentally. The question is still whether there is some information that can be obtained from the Von Neumann Entanglement Entropy that cannot be gleaned from the Shannon Entropy.

When we looked at the dynamics, we saw that our models, even the integrable one, exhibit very fast dynamics when taken far from equilibrium. We saw the fastest decay of the survival probability for full random matrices, where the decay is related to a Bessel function. The survival probability of realistic models is slower, but still Gaussian, which is faster than exponential. Several previous studies of quantum many-body systems suggested that the fastest decay of the survival probability should be exponential. They also tried to equate fast dynamics with chaotic systems. However, we verified that the decay of the survival probability can be faster than exponential even for integrable systems, whenever the systems are taken abruptly out of equilibrium. We also saw that the Shannon Entropy increases linearly for all of our models, indicating an exponential spreading of the initial state, which is another indication of very fast dynamics.

Hopefully, our work will be a step forward in understanding the nature of many-body quantum systems far from equilibrium, and will assist us in developing the technological wonders of the future.

VIII. ACKNOWLEDGMENTS

I would like to thank my faculty mentor, Dr. Lea Santos, for all of her guidance over the past two years. I would also like to thank Dr. Gabriel Cwilich, the previous director of the honors program, and Dr. Shalom Holtz, the current director, for all of their assistance throughout the thesis writing process. Additionally, I would like to thank Dr. Henry Kressel and the Kressel Scholarship Committee for providing me with the Kressel Undergraduate Research Fellowship for this past year. Finally, I would like to thank the National Science Foundation for providing funding (grant No. DMR-1603418) for my trip to the American Physical Society's March Meeting in New Orleans, where I presented some of our results.

IX. APPENDIX: PYTHON CODES

A. Basis

The following function can be used to generate a list of basis vectors for a case of N sites:

```
import itertools
def basis_full(N):
    return list(itertools.product([0,1], repeat = N))
```

If the number of excitations is conserved, then the basis for the subspace with N sites and r excitations can be found with the following function:

```
def basis_sub(N, r):
    output = []
    for indices in itertools.combinations(range(N), r):
        vector = [0] * N
        for index in indices:
            vector[index] = 1
        output.append(vector)
    return output
```

B. Hamiltonian

The following function gives the Hamiltonian matrix for the Heisenberg model:

```
import numpy as np
#basis = list of site basis vectors
#delta = anisotropy parameter
#lmda =  stregnth of NNN couplings relative to J
#defects = list of defect magnitudes on each site


def hamiltonian(basis, delta, lmda, defects):
    m = len(basis)
    n = len(basis[0])
    H = np.zeros((m,m))
    for i in range(m):
        for j in range(n-1):
            if basis[i][j] == basis[i][j+1]:
                H[i][i] += delta/4
            else:
                H[i][i] -= delta/4
                swapped = copy.copy(basis[i])
                swapped[j], swapped[j+1] = swapped[j+1], swapped[j]
                H[i][basis.index(swapped)] += .5

        #include if there are NNN coupings:
        for j in range(n-2):
            if basis[i][j] == basis[i][j+2]:
                H[i][i] += lmda*delta/4
            else:
                H[i][i] -= lmda*delta/4
                swapped = copy.copy(basis[i])
                swapped[j], swapped[j+2] = swapped[j+2], swapped[j]
                H[i][basis.index(swapped)] += .5*lmda

        #include if there are defects
            for j in range(n):
                if basis[i][j] = 1:
                    H[i][i] += defects[j]/2
                else:
                    H[i][i] -= defects[j]/2

        #include for closed boundary coditions:
        if basis[i][-1] == basis[i][0]:
            H[i][i] += delta/4
        else:
            H[i][i] -= delta/4
            swapped = copy.copy(basis[i])
            swapped[-1], swapped[0] = swapped[0], swapped[-1]
```

```
            H[i][basis.index(swapped)] += .5

        #include if there are both closed boundary coditions and NNN couplings
        if basis[i][-1] == basis[i][1]:
            H[i][i] += lmda*delta/4
        else:
            H[i][i] -= lmda*delta/4
            swapped = copy.copy(basis[i])
            swapped[-1], swapped[1] = swapped[1], swapped[-1]
            H[i][basis.index(swapped)] += .5*lmda
        if basis[i][-2] == basis[i][0]:
            H[i][i] += lmda*delta/4
        else:
            H[i][i] -= lmda*delta/4
            swapped = copy.copy(basis[i])
            swapped[-2], swapped[0] = swapped[0], swapped[-2]
            H[i][basis.index(swapped)] += .5*lmda

    return H
```

C. Wavefunction

The following function can be used to find the wavefunction in the site basis or the probabilities of measuring the site basis vectors.

```
import numpy as np
#basis = list of site basis vectors
#H = Hamiltonian matrix
#init = initial state
#times = list of times at which to calculate the wavefunction or probabilities

def wavefunction(basis, H, init, times):
    n = len(H)
    tl = len(times)
    eigen = np.linalg.eigh(H)
    wavefunction = np.empty((n, tl), dtype = 'complex128')
    #probabilities = np.empty((n,tl))
    init_index = basis.index(init)
    for i in range(n):
        total = np.zeros(tl, dtype = 'complex128')
        for j in range(n):
            total += eigen[1][init_index][j]*eigen[1][i][j] \
            *np.exp(-1j*eigen[0][j]*times)
        wavefunction[i] = total
        #probabilities[i] = abs(total)**2
    return wavefunction
    #return probabilities
```

D. Unfolding

1. Simple Approach

```
import numpy as np
#evals = eigenvalues
#fc = fraction of eigenvalues cut off each end
#group_size  = size of each group of eigenvalues
def simple_unfold(evals, fc, group_size):
    D = len(evals)
    cut = int(fc*D) #number of eigenvalues cut off each end
    cut_evals = evals[cut:(D-cut)]
    spacings_size = group_size - 1 #number of spacings in each group
    Dcut = len(cut_evals)
    if Dcut % spacings_size == 0:
        groups = Dcut/spacings_size - 1 #number of groups
    else:
        groups = Dcut/spacings_size
    avgs = [(cut_evals[(i+1)*spacings_size] - cut_evals[i*spacings_size])\
        /spacings_size for i in range(groups)]
    Dspaces = groups*spacings_size
    scaled_spacings = [(cut_evals[i+1]-cut_evals[i])/avgs[i/spacings_size]\
         for i in range(Dspaces)]
    unfolded_evals = np.zeros(Dspaces+1)
    for i in range(Dspaces):
        unfolded_evals[i+1] = unfolded_evals[i] + scaled_spacings[i]
    return unfolded_evals
```

2. Sophisticated Approach

```
import numpy as np
def sophisticated_unfold(evals, fc):
    D = len(evals)
    ncut = int(fc*D) #number of eigenvalues cut off each end
    cut_evals = evals[ncut:D-ncut]
    Dcut = D - 2*ncut

    eta = np.arange(Dcut) + 1

    p = np.polyfit(cut_evals, eta, 15)
    xi = lambda E: np.sum([p[i]*E**(15-i) for i in range(16)])
    xi = np.vectorize(xi)

    unfolded_evals = xi(cut_evals)
    return unfolded_evals
```

E. Shannon Entropy

1. Shannon Entropy of Eigenvectors

```
#D = dimension of matrix
#evecs = numpy array with eigenvectors as columns
import numpy as np
shannon = np.empty(D)
for i in range(D):
    evec = evecs[:,i]
    shannon[i] = -np.sum(abs(evec)**2 * np.log(abs(evec)**2))
```

2. Dynamic Shannon Entropy

```
#times = array of times at which to calculate the Shannon Entropy
#D = dimension of system
#evals = array of eigenvalues
#evecs = 2D array with eigenvectors as columns
import numpy as np
tl = len(times)
Wk = np.empty((tl, D))
for i in range(D):
    C = evecs[i]
    for l in range(tl):
        t = times[l]
        Wk[l, i] = abs(np.sum(C*initial_state *\
         np.exp(-1j*evals*t)))**2 + 10**-20
dynamic_shannon = -np.sum(Wk*np.log(Wk), axis = 1)
```

F. Entanglement Entropy

```
import numpy as np
def vonNeumann(basis, state):
    m = len(basis) #dimension of original matrix
    n = len(basis[0])
    sites = np.flipud(np.arange(n/2,n))
    short_basis = [] #basis vectors with those sites taken out
    new_basis = [] #short basis without duplicates
    removed_parts_per_vector = [] #part removed from each basis vector
    removed_parts = [] #unique parts removed
    for vector in basis:
        short_vector = copy.copy(vector)
        removed = []
        for site in sites:
            removed.insert(0,short_vector.pop(site))
        short_basis.append(short_vector)
        removed_parts_per_vector.append(removed)
        if not short_vector in new_basis:
            new_basis.append(short_vector)
        if not removed in removed_parts:
            removed_parts.append(removed)

    D = len(new_basis) #dimension of new matrix
    reduced_density_matrix = np.zeros((D,D), dtype = 'complex128')
```

```
    for removed_part in removed_parts:
        for i in range(m):
            if removed_parts_per_vector[i] == removed_part:
                for j in range(m):
                    if removed_parts_per_vector[j] == removed_part:
                        k = new_basis.index(short_basis[i])
                        l = new_basis.index(short_basis[j])
                        reduced_density_matrix[k,l] += state[i]\
                *np.conj(state[j])
    eig = np.linalg.eigh(reduced_density_matrix)
    ln_evals = np.log(eig[0] + 10**-20)
    ln_rdm = eig[1].dot(np.diag(ln_evals)).dot(eig[1].T.conj())
    von_neumann_entropy = np.real(-np.trace(np.dot(\
    reduced_density_matrix, ln_rdm)))
    return von_neumann_entropy
```


[1] D. Griffiths, *Introduction to Quantum Mechanics* second ed. Pearson Prentice Hall, (2005).

[2] R. Kubo, *Statistical-Mechanical Theory of Irreversible Processes. I. General Theory and Simple Applications to Magnetic and Conduction Problems*, J. Phys. Soc. Jpn. **12**, pp. 570-586 (1957)

[3] J. Eisert, M. Friesdorf, and C. Gogolin, *Quantum many-body systems out of equilibrium*, Nature Phys. **11**, 124–130 (2015).

[4] M. Greiner and S. Fölling, *Condensed-matter physics: Optical lattices*, Nature **453**, 736-738 (2008).

[5] P. Jurcevic, B. P. Lanyon, P. Hauke, C. Hempel, P. Zoller, R. Blatt, and C. F. Roos, *Quasiparticle engineering and entanglement propagation in a quantum many-body system*, Nature **511**, 202 (2014).

[6] P. Richerme, Z.-X. Gong, A. Lee, C. Senko, J. Smith, *Non-local propagation of correlations in quantum systems with long-range interactions*, Nature **511**, 198 (2014).

[7] Michael A. Nielsen and Isaac L. Chuang, *Quantum Computation and Quantum Information*, (Cambridge Press, Cambridge, 2010).

[8] Kira Joel, Davida Kollmar, and Lea F. Santos, *An introduction to the spectrum, symmetries and dynamics of spin-1/2 Heisenberg chains*, Am. J. Phys. **81**, 450-457 (2013).

[9] L. F. Santos, *Introduction to the computational analysis of static properties and dynamics of one-dimensional spin-1/2 systems* (2014) in `http://yu.edu/uploadedFiles/Faculty/Lea_Ferreira_dos_Santos/Computer_Codes/Izmir2014_04%282%29.pdf`.

[10] A. Gubin and L.F. Santos, *Quantum chaos: An introduction via chains of interacting spins 1/2*, Am. J. Phys. **80** 246–251 (2012).

[11] K. Winkler, G. Thalhammer, F. Lang, R. Grimm, J. H. Denschlag, A. J. Daley, A. Kantian, H. P. Büchler, and P. Zoller, *Repulsively bound atom pairs in an optical lattice*, Nature **441** 853 (2004).

[12] L. F. Santos and M. Dykman, *Quantum interference-induced stability of repulsively bound pairs of excitations*, New J. Phys. **14** 095019 (2014).

[13] K. Alligood, T. Sauer, and J. Yorke. *Chaos: An Introduction to Dynamical Systems.*, Springer-Verlag, (1996)

[14] T. Guhr, A. Mueller-Groöeling, H.A. Weidenmüller. *Random Matrix Theories in Quantum Physics: Common Concepts*, Phys. Rep. **299**, 189 (1998).

[15] F. C. Alcaraz, M. N. Barber, M. T. Batchelor, R. J. Baxter, and G. R. W. Quispel. *Surface exponents of the quantum XXZ, Ashkin-Teller and Potts models.* J. Phys. A 20, 6397 (1987).

[16] M. L. Mehta, *Random matrices*, Academic Press, San Diego, CA (2004)

[17] E.J. Torres-Herrera, J. Karp, M. Távora, L.F. Santos, *Realistic Many-Body Quantum Systems vs. Full Random Matrices: Static and Dynamical Properties*, Entropy, **18**, 359 (2016).

[18] J.J. Sakuri and J. Napolitano. *Modern Quantum Mechanics* second ed. Pearson Education, (2011).

[19] E. J. Torres-Herrera and L. F. Santos. *Dynamical Manifestations of Quantum Chaos: Correlation Hole and Bulge.* arXiv:1702.04363, (2017).

[20] A. Lagendijk, B. van Tiggelen, and D. S. Wiersma. *Fifty years of Anderson localization.* Physics Today 62, 24 (2009).